POU3f2 in human gliomas

-Expression pattern and functional role

Seyed Mohammad Lellahi

This thesis is submitted in partial fulfilment of the requirements for the degree of Master in Medical Biology

Translational Cancer Research Group-Department of Biomedicine

University of Bergen

Spring 2014

ACKNOWLEDGEMENTS

The present work was carried out at the Department of Biomedicine, Faculty of Medicine and Dentistry, The University of Bergen from March 2013 until May 2014.

First of all I would like to thank my main supervisor Prof. Per Øyvind Enger to whom I am deeply grateful to for excellent guidance, support, encouragement and teaching me how to think in a scientific manner. Even with a tightly packed schedule, you always managed the time for helpful guidance throughout this period.

I am also grateful to my co-supervisor Mohummad Aminur Rahman for his support, advice and for teaching me during my master thesis. I always met a smiling face when I came to your office with all my questions, and without your supervision and constant help this dissertation would not have been possible.

I am thankful to all members of the Oncomatrix Research Lab for all their scientific advice, patience and support, especially, Lina Wik Leiss and Halala Sdik Saed. I also wish to express my gratitude to Martha Chekenya Enger and Ercan Mutlu for helping me with the calculation of statistics. I would like to thank Per Øystein Sakariassen for helping me with designing. I am also grateful for all the help I have received from the technicians in the Translational Cancer Research group.

I would like to express my gratitude for all the help and support I received from my best friend Seyed Esmaeil Dorraji and my dear cousin Soraya Assarpour.

Many thanks go to dear Niloufar who always supported me and has shown a lot of understanding throughout this thesis.

Last but not least I would like to thank my wonderful family, my mother, my father, my beautiful sister and energetic brother, for their love, support and encouragement, particularly my mother for believing in me and pushing me for a better future.

Bergen, May 2014

Seyed Mohammad Lellahi

Summary

Gliomas are tumors of the central nervous system (CNS). They are responsible for about 28% of all central nervous system tumors and for 80% of all malignant brain tumors. The most commonly used classification and grading of CNS tumors is the World Health organization (WHO) classification: According to the WHO classification, gliomas are divided into four grades, from grade I to IV. Furthermore, different grade tumors are characterised by different genetic aberrations and phenotypes.

Tumor and fetal development display a resemblance due to the fast increase in biomass and extensive cell migration that characterised both processes. Thus the early embryo and tumors may share a common genetic basis. POU domain transcription factors have a critical role in embryo development, and reexpression/overexpression of these transcription factors have been reported in many cancers. POU3f2 is an intronless member of class III POU domain transcription factors. Its expression is confined to the CNS where it is involved in differentiation of neuronal and glial cell lineages in the embryo. Re-expression of POU3f2 has been reported in melanoma cancer by several independent groups. Although POU3f2 expression in gliomas has been sporadically reported, it has not been systematically characterised in a larger panel of gliomas of different grades and histologies. Since melanocytes and the main CNS cell types share a common neuroectodermal origin therefore, we hypothesized that POU3f2 is expressed in human gliomas.

In order to assess the expression of POU3f2 in glioma patients, and its possible correlation with malignancy grade, 51 formalin fixed paraffin embedded patient biopsies (grade II-IV) were stained by immunohistochemistry. Secondly, to confirm IHC results, western blotting and qRT-PCR were performed on about 40 human glioma biopsies. In addition, we conducted a series of experiments *in vitro* and *in vivo* to investigate how POU3f2 impacted on various aspects of glioma cell behavior.

We found that, POU3f2 is expressed in all grades of glioma of both astrocytic and oligodendroglial lineages. Moreover, expression was higher in grade IV than grade II tumors, whereas over-expression of POU3f2 in the U251cell line increased both glioma cell proliferation and colony formation. Conversely, down-regulation of POU3f2 decreased colony formation. Finally, over-expression of POU3f2 in the U251cell line promoted tumor

growth in nude mice, compared to U251 glioma cells with down-regulation of POU3f2 or expression of scrambled RNA sequences.

My plan for future studies will be to expand the present data to include additional glioma cell lines. In addition, my goal is to establish which signaling pathway mediates the effects of POU3f2.

ABBREVIATIONS

ABC	Avidin-Biotin complex
^{18}F-FLT	3'-Deoxy-3'-(18)F-fluorothymidine
Akt	Protein Kinase B (PKB)
ASCL1	Achaete-scute homolog 1
BBS	N,N-bis[2-hydroxyethyl]-2-aminoethanesulfonic acid -buffered saline
bp	base pair
Brn	Brain-specific homeobox/POU domain protein
BSA	Bovine Serum Albumin
CBTRUS	Central Brain Tumor Registry of the United States
CCNU	Lomustine
CDK4	Cyclin-dependent kinase 4
cDNA	Complementary DNA
cm^2	Square centimetre
CNS	Central Nervous system
CRH	Corticotropin Releasing Hormone
CT	Contrast-enhanced computerized tomography
Ct	Cycle of threshold
DAB	3,3'-diaminobenzidine
DAPI	4', 6'-Diamidino-2-phenylindole
DGC	Differentiated glioblastoma cells
dH2O	Distilled water
DMEM	Dulbeccos Modified Eagles Medium
DMSO	Dimethyl Sulfoxide
DNA	Deoxyribonucleic acid
E	Embryonic day
E.coli	Escherichia coli
EDTA	Ethylenediaminetetraacetic acid
EGFR	Epidermal growth factor receptor
ESC	Embryonic stem cells
FACS	Fluorescence activated cell sorting
FLAIR	Fluid-attenuated inversion recovery
FoxG1	Forhead box protein
FW	Forward
GAPDH	Glyceraldehyde-3-phosphate-dehydrogenase
GBM	Glioblastoma multiforme
GFP	Green fluorescent protein
GH	Growth hormone
GnRH	Gonadotropin-releasing hormone
HEK 293 cells	Human Embryonic Kidney 293 cells
HIER	Heat induced epitope retrieval
HRP	Horseradish peroxidase

HTH	Helix-turn-helix
IARC	International Agency for Research On Cancer
ICC	Immunocytochemistry
ICM	Inner cell mass
IDH1	Isocitrate dehydrogenase 1
IHC	Immunohistochemistry
iNPC	Induce neural precursor cells
iTPC	Induced stem-like tumor propagating cells
Kda	Kilodalton
Ki-67	Antigen Ki-67
LB agar	Lysogeny broth agar
LI	Labeling index
LOH	Loss of heterozygosity
MDM2	Mouse double minute 2 homolog
MIC	Molecular imaging centre
mm^2	Square millimetre
mm^3	Cubic millimeter
MRI	Magnetic resonance imaging
mTOR	Mechanistic target of rapamycin
MYt1l	Myelin Transcription Factor 1-Like
NANOG	Nanog homeobox
NEB	New England Biolabs
nm	Nanometre
NOS	Not Otherwise Specified
O.C.T	Optimal cutting temperature compound
Oct	Octamer binding transcription factor
OLIG2	Oligodendrocyte lineage transcription factor 2
OX	Overexpressor
P	Short arm of chromosome
P	P-value
P16INK4a	Inhibitor of kinase 4a/CDKN2A
P19	Embryonic carcinoma cell lines
PA	Pilocytic astrocytomas
PBS	Phosphate buffered saline
PCR	Polymerase chain reaction
PDGFR	Platelet-derived growth factor receptors
PET	Positron emission tomography
PI3K	Phosphatidylinositol-4,5-bisphosphate 3-kinase
pit1	Pituitary-specific positive transcription factor 1
PNS	Peripheral nervous system
POU3f2	POU class 3 homeobox 2
POU_H	POU-homeo
POU_S	POU- specific
PRL	Prolactin

PTEN	Phosphatase and tensin homolog
q	Long arm of choromosome
qRT-PCR	Quantitative polymerase chain reaction
Raf	Rapidly Accelerated Fibrosarcoma
RAS	Rat sarcoma
RB	Retinoblastoma
REV	Reverse
RFU	Relative fluorescence units
RNA	Messenger Ribonucleic acid
rpm	Rounds per minute
RT	Room temperature
SALL2	Spalt-like transcription factor 2
SCLC	Small cell lung cancer
SDS	Sodium dodecyl sulfate
SDS-PAGE	Sodium dodecyl sulfate polyacrylamide gel
SE	Standard error
SEM	Standard error of the mean
siRNA	Small interfering RNA
SOC medium	Super Optimal broth with Catabolite repression medium
SOX	Sex determing region Y-box
TAE	Tris-acetate-EDTA
TBS	Tris buffered saline
TBST	Tris-buffered saline and Tween 20
TF	Transcription factor
TMZ	Temozolomide
TP53	Tumor protein p53
TPCs	Tumor propagating cells
Tris	Tris (hydroxymethyl) aminomethane
TSH	Thyrotropes
UV	Ultra violet
WB	Western blotting
WHO	World Health organization
Wnt	Wingless-type MMTV integration site protein
WT	Wild type

Table of contents

1. Introduction

1.1 Cancer

1.1.1 Cancer

Cancer is characterized by dysregulated and increased cell division resulting from a sequential acquisition of DNA changes[1,2]. Thus, cancer has been characterised as a disease of the genome since it invariably displays some form of genetic aberration, including mutations and chromosomal rearrangements which dictate clinical behavior[3,4]. Typically these changes involve oncogenes and tumor suppressors. The oncogenes accelerate cell growth while tumor suppressors have the opposite effect. Therefore, gene alterations that increase oncogene activity or decrease tumor suppressor activity may promote cell proliferation[5]. Generally, one single cell is the origin of the cancer through clonal growth. The resulting tumor can invade nearby tissues, and may also spread to other organs[6]. Any part of the body can be affected by cancer[6]. In 2012, 8.2 million deaths were attributed to cancer with lung, liver, stomach, colorectal and breast cancer being the cause of most cancer deaths in all the world[6]. Genetic inheritance is the cause of 5-10% of all the cancers, whereas in 90-95% of the cases, environment and lifestyle (cigarette smoking, diet, alcohol, sun exposure, pollutants, infections, stress, and obesity) are held responsible. Thus, life style changes may be the most effective strategy to reduce the incidence of cancer[7].

1.1.2 Cancer - hallmarks

Cancer is a progressive disease; the normal cell undergoes a multistep process to acquire the features of a cancer cell. Six physiologic changes (also called hallmarks) which are necessary for malignant growth have been suggested by Hanahan and Weinberg (Fig 1.1.2). Self-sufficiency in growth signals is the first hallmark; normal cells need mitogenic growth signals for proliferation. In many cancers, normal growth signaling is mimicked by oncogenes[8,9]. In normal cells, cellular quiescence and tissue homeostasis are maintained by various anti-proliferative signals inhibiting growth via transmembrane cell surface receptors. Conversely, cancer cells are often insensitive to antigrowth signals (second hallmark)[8]. In addition, their ability to evade apoptosis (third hallmark) also increases overall tumor

growth[8], whereas disruption of cell-to-cell signaling and aberrant telomerase expression contribute to a limitless replicative potential (fourth hallmark)[8]. Without blood circulation, cancer cells grow up to 1-2 mm^3 in diameter, but for further development (beyond $2mm^3$) angiogenesis (fifth hallmark) is necessary for tumor growth[10], and is mediated by the release of vascular endothelial growth factor (VEGF) from the tumor cells. Tissue Invasion and Metastasis constitute the sixth hallmark of cancer: If untreated, primary malignant tumors will at some point invade nearby tissue and spread to distant sites of the body, which is the cause of 90% of cancer-related deaths. Recently, Hanahan et al also proposed that the

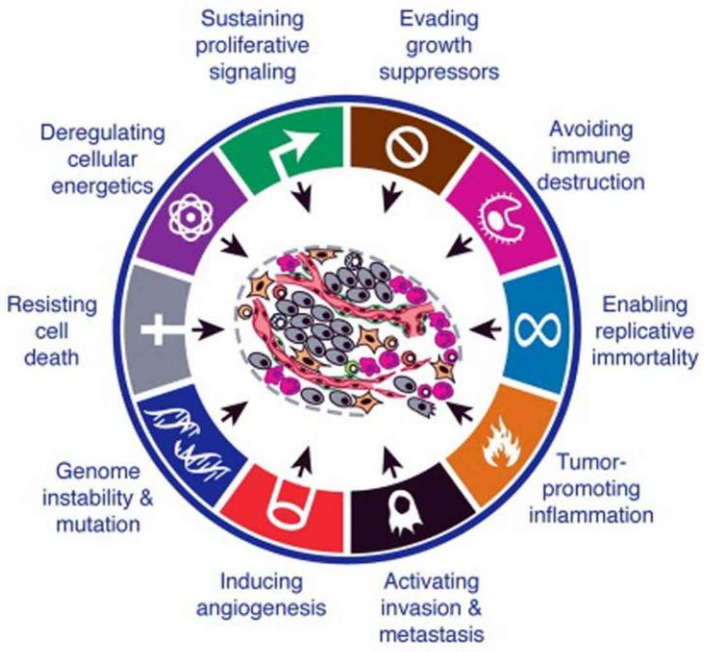

Figure 1.1.2 Hallmarks of cancer. The six hallmarks introduced by Hanahan and Weinberg in 2000. Two enabling characteristics and two emerging hallmarks were later proposed (Reprinted with permission).

reprograming of energy metabolism could be cited as "Emerging Hallmarks" (Fig 1.1.2)[9]. The energy needed for cell proliferation is for a large part obtained by elevated glycolysis and lactate production even under aerobic conditions (Warburg effect)[9]. Another emerging hallmark that has been proposed, is the evasion of immune destruction by cancer cells[9]. Genome instability has been seen as an enabling characteristic through random mutations and chromosome rearrangement leading to the acquisition of the multiple hallmarks[9]. Furthermore, inflammation can have a tumor-promoting role by providing bioactive molecules to the tumor microenvironment. Inflammatory changes is often mediated by

immune cells that supply growth factors, survival factors, proangiogenic factors and matrix-modifying enzymes[9]. Since these hallmarks are considered necessary for malignant transformations, they may also be therapeutic targets. However, cancer cells often respond with compensatory changes, and can reduce their dependence on specific hallmarks while using others during cancer progression[9].

1.1.3 Gliomas- classification, grading and epidemiology

Gliomas are tumors of the central nervous system (CNS) in which the neoplastic cells display a glial phenotype. They account for about 28% of all central nervous system tumors and 80% of all malignant brain tumors[11]. The current glioma classification is based on the tumor cells' resemblance to the main glial cell types[12,13], whereas tumors are graded on their degree of malignancy[14]. This grading is based on histological changes such as the presence of nuclear pleomorphism, mitotic activity, endothelial cell proliferation and necrosis[11,15].

Table 1.1.3 Astrocytoma grading according to the World Health Organization (WHO) classification. Modified from WHO classification[5].

Astrocytic tumor	Grading	Criteria
Pilocytic Astrocytoma	**I**	Slow proliferation
Diffuse Astrocytoma	**II**	Infiltrative, slow proliferation, nuclear atypia
Anaplastic Astrocytoma	**III**	Infiltrative, mitotic activity, nuclear atypia, anaplasia
Glioblastoma Multiforme	**IV**	Highly infiltrative, mitotic activity, nuclear atypia, endothelial proliferation, necrosis

According to the WHO classification, gliomas are classified from grade I that are considered benign to grade IV, the most aggressive tumors[16,5]. Notably, the different grades correlate with different prognoses and treatment guidelines are also based on tumor grade[15,17]. The classification for astrocytic tumors are shown in table 1.1.3[12,17]. Grade II astrocytoma typically display nuclear atypia[18]. Patients with grade II have a 5-year survival rate of approximately 50%.[5,11]. Grade III is characterized by nuclear atypia and mitotic activity. Patients with grade III tumors survive 2-5 years[5]. Both grade II and III tumors are infiltrative in nature[15] and have a propensity for malignant progression to a higher grade[5,19,20]. GBM is a grade IV tumor showing all the traits of grade II-III tumors plus necrosis and vascular proliferation[15], and median survival is 15 months[21,22]. Tumors with none of these features are

grouped as grade I[18]. Grade I is assigned to the more circumscribed pilocytic astrocytoma[15], this tumor is the most common glioma in children with excellent prognosis after tumor removal[19,23].

The relative frequency of different glioma types is illustrated in figure 1.1.3. Apart from astrocytomas other important types of gliomas are oligodendroglioma, mixed oligoastrocytoma and ependymoma[11]. Oligodendrogliomas constitute about 6.1% of all gliomas[24]. According to the WHO grading system, oligodendrogliomas are divided into grade II (oligodendrogliomas) and grade III (anaplastic oligodendrogliomas) tumors. Oligodendrogliomas are infiltrative and usually arise in adults, in the age range 50-60 years[5]. The mixed oligoastrocytomas have features of both astrocytoma and oligodendroglioma[5,11]. Ependymomas are usually slow growing and typically occur in children and young adults. It originates from the wall of the cerebral ventricles and spinal canal[5].

According to the International Agency for Research On Cancer (IARC), the incidence rate (new cases/100 000/year) of brain tumors globally was 3.4 in 2012 (5-years prevalence) with 3.9 for men and 3.0 for women[25]. The incidence of brain tumors is higher in developed

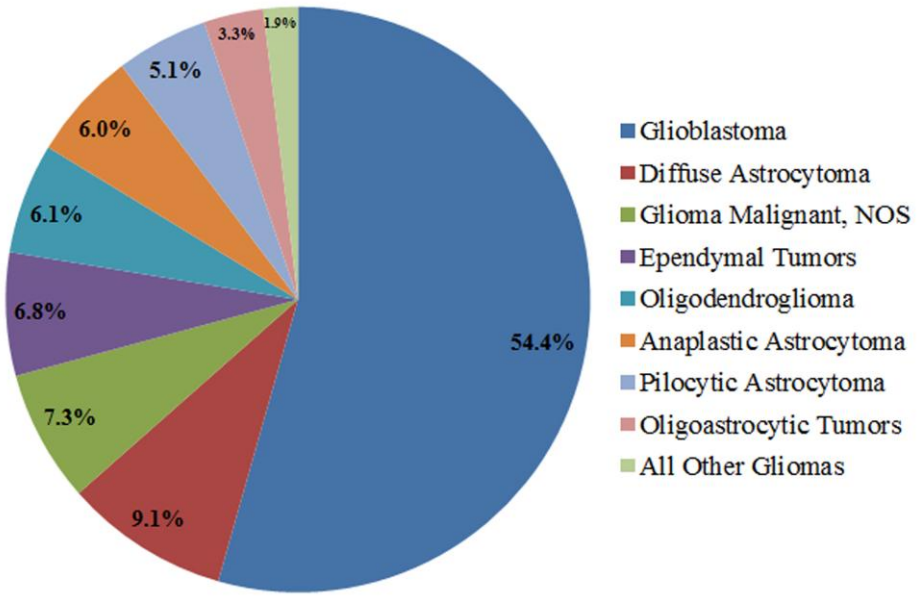

Figure 1.1.3 Distribution of Primary Brain and CNS gliomas by histology subtypes. This data was collected from 2005 to 2010 in the United States of America[24].

countries than in less developed countries[26]. According to the Central Brain Tumor Registry of the United States (CBTRUS) between 2006 to 2010, the incidence rate of glioma was 7.14 for men and 5.06 for women[24]. The incidence of gliomas is twice as high in Caucasians compared to Africans[24]. In addition, the frequency of gliomas is higher in men than women[24,27]. Glioblastoma is the most common glioma (54.4% of all gliomas) while astrocytoma and glioblastoma are responsible for about 75% of all gliomas (Fig 1.1.3).

1.1.4 Genetic progression in gliomas

Gliomas are genetically heterogeneous although some genetic changes are associated with histological subtypes or different grades (Fig 1.1.4). Mutations in TP53 and IDH1 are among the earliest genetic aberrations in grade II astrocytoma and are also seen in secondary glioblastomas[11]. About 25% of grade II astrocytomas however, are not TP53 mutated and display other genetic alterations such as gain of chromosome 7q and amplification of 8q[5].

Genetically, anaplastic astrocytoma represent an intermediate stage in glioma progression[5]. The rate of TP53 mutation is high in anaplastic astrocytomas (53%)[5,28] as in astrocytomas. Other important mutations are IDH1/2 mutation (about 80%)[29], p16 deletion (~ 30%), RB mutation (25%), $p19^{ARF}$ deletion (15%), CDK4 amplification (10%), LOH on chromosome 10q (30%), LOH on chromosome 19q (~ 40%), LOH on 22q (~ 30%)[5] (Fig 1.1.4).

Glioblastoma multiforme (GBM) (grade IV) may develop *de novo* (primary GBM) or arise from a lower grade glioma (secondary GBM). Primary GBMs develop at older age (mean age 62 years), while secondary GBMs develop in younger patients (mean age 45 years)[30]. Primary and secondary GBMs display both overlapping and distinct genetic changes[28] (Fig 1.1.4). LOH of 10q is the most genetic aberration in both primary and secondary GBMs. PTEN inactivation and EGFR amplification are the most frequent genetic alterations in primary GBMs, while TP53 mutation occurs more frequently in secondary GBMs [31,32]. The MDM2 amplification/overexpression is more common in primary GBMs without a TP53 mutation, while overexpression of MDM2 mutation in secondary GBMs is about 10% [28]. The rate of LOH on chromosome 19 is higher in secondary GBMs (54%) in comparison to primary GBMs (6%)[28]. The incidence of IDH1 mutation in secondary glioblastoma (88%) is higher than primary glioblastoma (7%)[33]. These genetic aberrations usually impact on changes in receptor tyrosine kinase signaling (88%), the TP53 (87%) and RB pathway (78%)[34].

Figure 1.1.4 Main genetic mutation in human glioma patients by different grade[135,53,37,28].

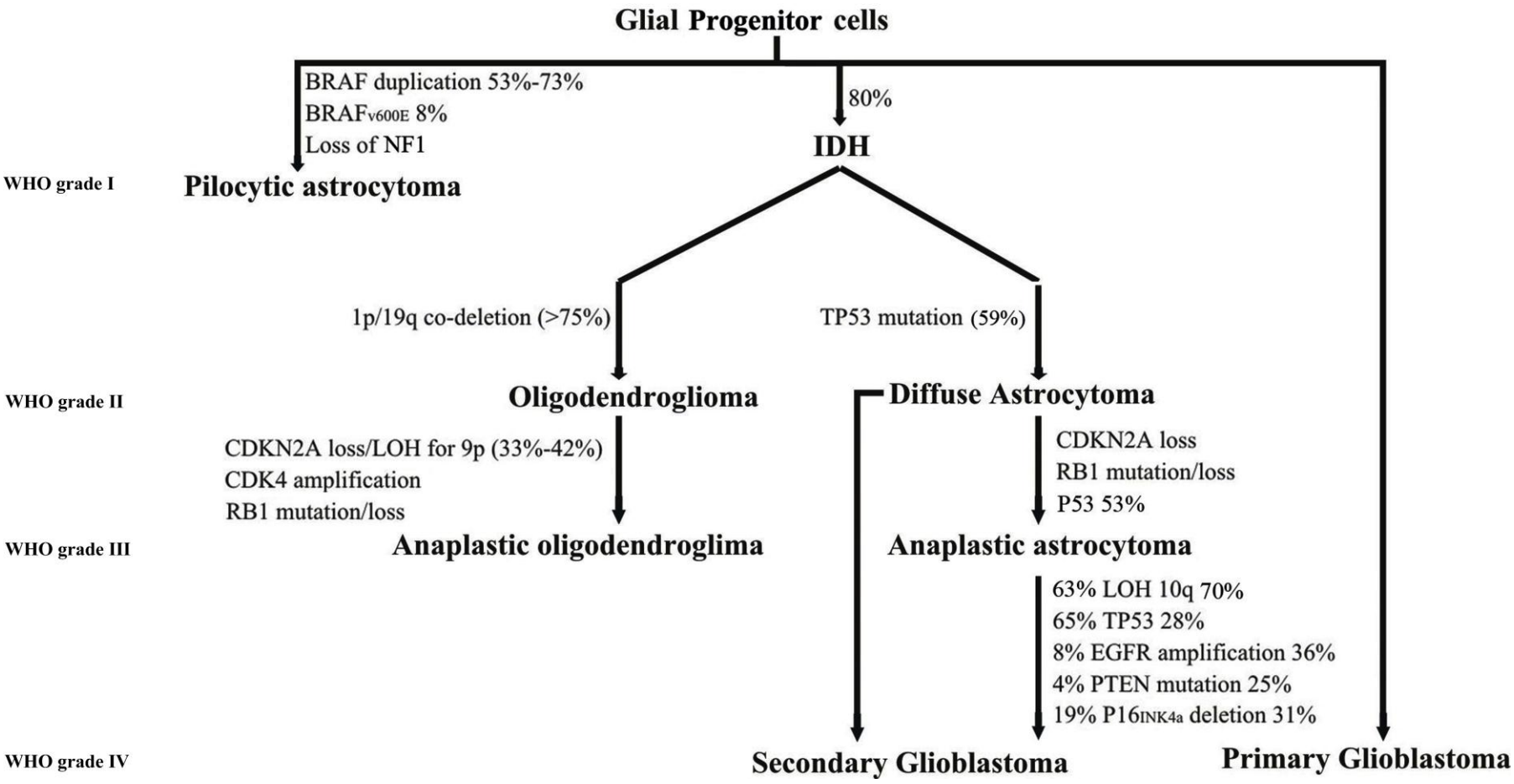

The pilocytic astrocytomas (PAs) display loss of chromosomes 17 or 17p and gain of 8q as the most frequent karyotype changes in PAs[35]. Mutation in the P53 gene is also reported in 0-35% of PAs cases[36] but it is not indicative of PAs[5].

Genetic aberrations in oligodendrogliomas are distinct from those observed in astrocytomas. Loss of heterozygosity (LOH) on 19q (50-80%) is the first and LOH of 1p (67%) is the second most frequent genetic change in Oligodendogliomas, whereas the rate of TP53 mutation is low[5]. Anaplastic oligodendrogliomas, display 19q and 1p deletions similarly to grade II oligodendroglioma, but often also have deletions of 9p and additional chromosomes (4, 6, 10, 11, 15 and 18)[5,37]. IDH1/2 mutations are observed in approximately 65% of oligodendroglioma[33,29].

1.1.5 Biology of gliomas and its implications for diagnosis, treatment and prognosis

1.1.5.1 General biology of gliomas

Proliferation: Immunostaining for the proliferation marker Ki-67 show that only approximately 4% of tumor cells in gradeII are actively cycling, whereas the fraction is usually in the range of 5-10% in anaplastic astrocytomas[5,38]. The rate of Ki-67 expression in GBM is even higher, typically 15-20%[5,38].

Angiogenesis: Angiogenesis is considered a key event in malignant glioma progression, accompanying the transition from grade III to grade IV tumors[39]. Normally, hypoxic conditions induce the release of angiogenic factors and down-regulation of anti-angiogenic factors[39]. GBMs usually are highly angiogenic, and typically display large dilated and malformed. Vessel formation is not present in grade II and III gliomas, although angiogenic factors are released in grade III gliomas[39].

Invasion: All grade II-IV gliomas are characterised by highly infiltrative growth[40]. Typically, glioma cells migrate along the white matter tracts, often to the contralateral hemisphere. They also infiltrate the cortex and in the subependymal zone. However, gliomas hardly ever metastasise outside the CNS[5,41].

1.1.5.2 Diagnosis

Diagnosis of glioma is based on clinical symptoms, neuroimaging and histopathological examination[5]. Glioma patients typically describe symptoms such as headache, seizure, mood and personality changes, vomiting, nausea, epilepsy, memory loss, confusion and visual changes[42,43,44,45,46]. These symptoms can either be ascribed to increased intracranial pressure or they result from invasion or compression of surrounding structures. MRI is currently the preferred method for diagnosing gliomas[47]. On contrast-enhanced T1-weighted MRI images, GBMs appear as a hypo-intense lesion surrounded by a contrasting-enhancing ring structure representing a disrupted blood-brain-barrier. On T2-weighted images and fluid-attenuated inversion recovery (FLAIR), tumors appear hyper-intense[48]. In anaplastic astrocytomas (WHO grade III) only modest contrast enhancement is usually observed. Grade II astrocytomas do not enhance, and the tumor area appear hypo-intense on T1-weighted images and hyper-intensity on T2-weighted images[5]. In patients that cannot undergo MRI, CT usually shows the area of contrast enhancement clearly, surrounding a hypo-dense area. Lower grade gliomas usually do not enhance and typically present as hypo-dense lesions although they can be difficult detect[5].

1.1.5.3 Treatment

The primary treatment for grade III and IV gliomas is usually surgery followed by radio- and chemotherapy[49]. In grade II gliomas the primary treatment is most often surgery alone[46].

Surgery: The goal of surgery in gliomas is to: (1) provide histological diagnosis, (2) relieve intracranial pressure (3) by gross removal of the tumor increase survival time of the patients[50]. As much tumor mass as possible is removed without causing neurological deficits[51]. Radical removal of gliomas is not possible due to their infiltrative growth. Gross total removal however, is correlated with longer survival and better quality of life[52]. In patients with pilocytic astrocytoma, surgical resection of the tumor is the first choice of treatment, and complete resection of the tumor results in a cure[53].

Radiotherapy: Fractionated radiotherapy is routinely administered for grade III and IV gliomas after surgery to a total of 54-60 Gray, and has been shown to prolong survival. This give in 30 fractions of 1.8-2 Gray over 6 weeks[54]. Patients over 70 years usually receive a lower dose due to side-effects[55]. In grade II tumors, with low mitotic labeling index,

radiotherapy is usually not given but may be considered with early recurrences or other signs of an aggressive disease course[49].

Chemotherapy: Temozolomide (TMZ) is now routinely given to patients with grade III and IV gliomas and has been shown to prolong survival[54,56]. TMZ is an alkylating agent which is administered orally and usually well tolerated[57]. It is given concomitantly with fractionated radiotherapy and then adjuvantly in five-days cycles every fourth week for a total of six times[58]. TMZ is not routinely administered for grad II gliomas[57].

Treatment of Oligodendrogliomas: LOH of 1p/19q chromosome has been established as a predictive marker for response to chemotherapy, and, Oligodendrogliomas are usually more chemosensitive than astrocytomas[59,56]. Both TMZ and PCV (procarbazine, CCNU, vincristine) are both in clinical use, and they are considered to be of similar anti-tumor efficacy[60,56]. In recent years, various biological therapies have been tested clinically, such as tyrosine kinases targeting the EGFR and PDGFR receptors, and inhibitors of mTOR and PI3K. However, a survival benefit has not been shown with any of these tratments[61,62].

1.1.6 Gliomas from a developmental perspective

Development of the fetus and tumor growth display a resemblance from a biological and molecular perspective[63]. Both processes are accompanied by extensive cell proliferation and migration[63]. Furthermore, several studies have shown that genes expressed in the embryo are aberrantly expressed in cancers[63,64]. Notably, pluripotent stem cells express the transcription factors Oct4, SOX2 and Nanog which are also expressed in gliomas[65,66]. In stem cells, these factors are important regulators of potency and self-renewal during development of the fetus. It is therefore possible that they have a similar role in gliomas[65]. Moreover, embryonic stem cells (ESCs) and gliomas show activation of the same signaling pathways, such as activation of the Notch signaling pathway and the Hedgehog signaling pathway[67].

1.2 POU3f2

1.2.1 The POU class of transcription factors – structure and function

The process of differentiation is tightly regulated by numerous transcription factors. The family of POU transcription factors is divided into six classes in mammalians[68]. In mammals, six classes of POU proteins have been described based upon amino acid sequence of the POU domain as well as the extent of linker region conservation[68]. Some POU transcription factors are expressed in specific cell types whereas others are expressed more broadly. They perform different functions such as regulation of house-keeping genes, and have a crucial role in the determination of the cells fate[68]. In addition, they are critical to neuronal cell function[69].The POU proteins bind promoters of other genes involved in DNA replication and development[68].The POU domain was first described in 1988[70] and was recognized by comparison of three mammalian transcription regulators, Pit 1, Oct1 and Oct 2

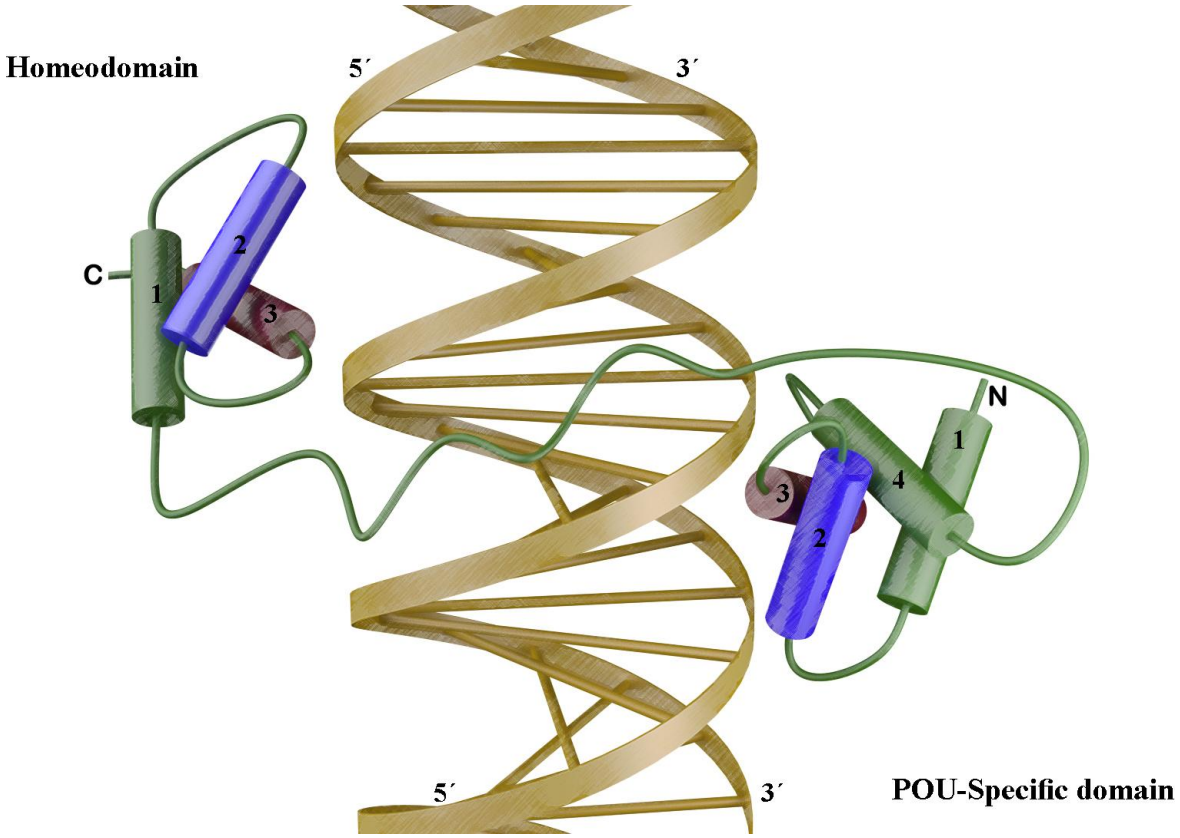

Figure 1.2.1 General structure of POU-domain. The POU-domain consists of both homeodomain (POU_H) and POU-specific domain (POU_S) which join to each other by flexible linker. The POU_H and POU_S bind to opposite sides of the DNA while are connected to each other by linker. The POU_S domain binds to the ATGC half site and the POU_H domain binds to the AAAT half site[74]. Drawn by Per Øystein Sakariassen.

with the Unc-86 gene from a nematode cell lineage called Caenorbabditis elegans[69,71,72]. POU domains have not been identified in fungi or plants[71]. The POU domain proteins are characterized by a conserved region that contains 150-160 amino acids[73]. The POU domain is bipartite and consists of two POU sub-domains, the POU- specific (POU_S) domain at the N-terminal which consists of 75-82 amino acids, and the POU-homeo (POU_H) domain at the C-terminal which consists of 60 amino acids (Fig 1.2.1). These subdomains are connected to each other by a lesser conserved linker region of 15 to 56 amino acids in length[69,74]. The POU_S and POU_H domains both have a helix-turn-helix (HTH) motif and are able to recognize and bind specific DNA sequences independently[71]. POU_S consists of four α-helices of which α1 and α4 stabilize the HTH motif whereas α3-helix is a DNA-recognition helix. The POU_H consists of three α-helices, in which α1 stabilizes the HTH while α3 is responsible for recognition of a specific DNA-sequence[71,73] (Fig 1.2.1).

The isolated POU_S bind to the specific sequences of DNA with very low affinity while the POU_H binds DNA with moderate affinity[75]. The POU domain transcription factors require both the POU_S and POU_H in order to bind to the specific site of DNA with high affinity[74]. The DNA sequence recognized by the POU domain is the 5´-ATGCAAAT-3´ octameric sequence. The protein crystallography of the Oct1 protein shows that both the POU_S and POU_H domains bind to the major groove of the DNA strand, but on the opposite sides of the DNA helix. The POU_S binds to the 5´-ATGC and the POU_H binds to the 3´-AAAT. The POU transcription factors are able to combine to other co-activators, co-repressors or other transcription factors from the same or other families in order to perform their activities[68]. The linker gives flexibility leading to differences in orientation of the half-site sequences that are bound by the POU_S and POU_H domains.

1.2.2 Regional expression patterns of POU transcription factors

The POU factors display different spatiotemporal expression patterns and execute various biological functions. Some members of the POU family are expressed ubiquitously, while others show a restricted spatial expression with a more limited function[69] (Table 1.2.3). They are expressed at different embryonal stages, and have critical roles during development. In adults, the POU transcription factors are generally not expressed, or at only low levels, except Oct1 (member of class II) which is expressed in many cell types[72] (Table 1.2.3). The

abundant expression of Oct1 and the presence of an octamer motif in the promoters of housekeeping genes suggest that Oct1 is a constitutive housekeeping transcription factor[76].

Oct4 (member of class V) and Oct6 (member of class III) have been identified in embryonic stem cells[69]. Oct4 is one of the earliest genes expressed from the zygote genome which is necessary for the generation of pluripotent embryonic stem cells[68] (Table 1.2.3). Oct4 specifies cell fate while its expression decreases after differentiation[77]. Cell fate decisions are highly sensitive to changes in Oct4 expression. Oct4 has a pivotal role in the ESCs fate, and they maintain the pluripotent potential of stem cells only when Oct4 is expressed in the physiological range. Conversely two fold overexpression triggers ESC differentiation into primitive endoderm and mesoderm, whereas a downregulation of Oct4 induces ESCs to differentiate into trophoblasts[68,77]. In adults, Oct4 mRNA expression is detected in the ovaries and testes[78,69] (Table 1.2.3). In addition, Oct4 mRNA and protein are observed in the oocyte but not in spermatocytes[79,80]. Initially, Oct4 is expressed throughout the blastomere, while it subsequently is confined to the inner cell mass (ICM) of the blastocyst.

Oct6 is expressed in early embryogenesis, similarly to Oct4 in the totipotent and pluripotent stem cells of the pre-gastrulation embryo. It is down-regulated during later development, although it remains expressed in specific developing neurons and is found in the adult brain and testes[81] (Table 1.2.3).

A significant number of the POU domain proteins, such as Tst1/Oct-6/SCIP, Pit1, Oct1, Oct2, Brn1, Brn2 (POU3f2), Brn4, Brn3a, Brn3b, and Brn5 are expressed primarily or exclusively in the nervous system[69,68,81]. The Pit1 transcription factor is a member of the Class I POU transcription factors (Table 1.2.3) and regulates pituitary development. Pit1 is necessary for final development of thyrotropes (TSH expression), lactotropes (prolactin (PRL) expression) and somatotropes (growth hormone (GH) expression)[76]. Animals that are not able to express Pit1, have hypoplastic pituitaries and lack somatotropes, lactotropes, and thyrotropes[74].

Oct2 is member of the class II POU domain which is widely expressed in neurons during embryonal development (Table 1.2.3). In adults, Oct2 expression is confined to the suprachiasmatic and medial mammillary nuclei, hippocampus, olfactory tract, olfactory bulb, lymphoid cells, testes and thymus[69,79].

Brn1, Brn2 (POU3f2), Brn4 and Tst-1/Pou3f1/SCIP (OCT6) are four intronless mammalian class III POU genes[74,82] (Table 1.2.3). Brn1, POU3f2 and Brn4 are expressed extensively in the nervous system at day 10 to 11. By day 14, Brn1 and POU3f2 are expressed in four separate regions in the hypothalamus (preoptic, anterior, ventromedial, and mammillary nuclei) while POU3f2 and Brn4 are co-localized in the paraventricular and supraoptic neurons[79]. Tst1/Pou3f1/SCIP is expressed in oligodendrocyte precursors and developing Schwann cells, and is responsible for myelination in the CNS and PNS.

Class IV POU domain proteins are structurally related to the UNC-86 gene product in C.elegans. Brn3a, Brn3c, and Brn3b are three members of the mammalian class IV which are expressed in the PNS and CNS[74] (Table 1.2.3).

Brn5 is a member of the class VI POU domain (Table 1.2.3). Brn5 is widely expressed in neurons as well as tissues outside the nervous system, including, kidneys, lungs, heart, adrenal gland, skin, testes, and anterior pituitary[79,83].

1.2.3 POU transcription factors - biological roles in health and disease

Normal development of the embryo requires a tightly regulated pattern of gene expressions, and deviations from this pattern are associated with phenotypical abnormalities[84]. Dysregulation of class III and class IV of the POU transcription factors lead to different deficiency (Table 1.2.3); in class III, Brn1 is essential in the development and function of the nephron in the kidney and it is able to regulate the androgen activity mechanism in kidneys[85]. Brn4 null mice have several defects in development of the inner ear causing deafness but there are no detectable defects in development/function of the CNS[79]. Also the knockout mice for class IV POU transcription factors, showed that most deficiencies impacted on the development of specific neuronal cell types, mainly leading to deficiency in ears and eyes[86]. The expression of POU domain transcription factors has been reported in different cancer types[69] (Table 1.2.3). Notably, expression of Oct4 has been reported in many somatic cancers such as gliomas, lung cancer, breast cancer, prostate cancer, non-small cell, bladder cancer, oral squamous cell carcinoma, gastric cancer, and esophageal cancer[64] (Table 1.2.3). Expression of Brn1(class III) and Brn3b (class IV) are also founded in breast cancer[87] (more examples are listed in table 1.2.3).

Table 1.2.3 POU transcription factors family: Regional expression in embryo and adult, knock out phenotype and cancers[79,69].

Class	POU factor and synonym	Expression in embryo	Expression in adult	Knock out phenotype	Cancer
I	**POU1F1 (Pit1)**	Pituitary gland, neural	Pituitary gland, breast	Lack of somatotropes, lactotropes and thyrotropes	Breast cancer
II	**POU2F1 (Oct1)**	Brain, neural crest	Ubiquitous	-	-
	POU2F2 (Oct2)	Neural crest	Neurons, lymphoid cells	Defective function of B lymphocytes	-
	POU2F3 (Oct11)	Epidermis	Testis, thymus	Deficiency of epidermal keratinocytes	Cervical cancer
III	**POU3F1 (Oct6)**	Stem cells, neurons	Brain, testis	Defective myelination	Hepatocellular carcinoma
	POU3F2 (Brn2)	Hypothalamus, pituitary	Hypothalamus, pituitary gland	Lack of CRH, vasopressin, and oxytocin neurons in paraventricular and supraoptic nucleus	Merkel cell carcinoma, lung cancer, neuroblastoma, Tcell lymphoma, melanoma
	POU3F3 (Brn1)	Neurons	Brain	-	Prostate cancer, adenoid cystic cancer, breast cancer
	POU3F4 (Brn4)	Neurons	Brain	Deafness	-
IV	**POU4F1 (Brn3a)**	Neural crest, PNS, CNS	Ganglia, CNS, breast, cervix, testis	Lack of certain sensory and autonomic	Ewing's sarcoma, neuroepithelioma, cervical cancer
	POU4F2 (Brn3b)	Neurons, retinal neurons	Retinal ganglia	Loss of retinal ganglion cells	Breast cancer, neuroblastoma, bladder cancer
	POU4F3 (Brn3c)	Neurons	Brain	Deafness	Merkel cell carcinoma
V	**POU5F1 (Oct4)**	Early embryonic cells, stem cells	Oocytes, testis	All cells in the early embryo become trophoblasts	Many type of cancer
	POU5F2 (Sprm1)	Neurons	Testis, brain	Reduce fertility	-
VI	**POU6F1 (Brn5)**	Nervous system	Nervous system	-	Ovary adenocarcinoma
	POU6F2 (Rpf1)	Retina, PNS	Retina, hypothalamus	-	Wilms tumor

1.2.4 POU3f2 – expression patterns and biological function

POU3f2 (Brain2, Brn2,N-Oct-3, Oct7) is an intron less member of the class III POU domain and is located on chromosome 6q16 in humans[74,68,88,89]. POU3f2 binds the octameric sequence of ATG(C/T)TAAT, but the majority of POU3f2 binding sites are a consensus non-octameric sequence ATG(A/C)AT(A/T)0-2ATTNAT[90]. In adults, expression of POU3f2 is restricted to the hypothalamus and part of the cortex[69] while it is expressed widely in the CNS during embryogenesis[74]. POU3f2 is a critical regulator of cell differentiation along neuronal and glial cell lineages[70]. Moreover, it is involved in the production and positioning of neocortical neurons[91,92]. In POU3f2-null mice, migratory precursor cell neurons of the paraventricular nuclei and supraoptic nuclei of hypothalamus die at E12.5[93]. The POU3f2 null mice are live born, but smaller in size compared to wild type mice[79]. Furthermore, they show severe malnutrition and decrease in brown adipose tissue, and usually die within day 10 after birth[74,79]. Moreover, POU3f2 is involved in the production and positioning of neocortical neurons[91,92]. POU3f2 is necessary for the differentiation of neurosecretory neurons in the posterior pituitary gland[69,76,94]. POU3f2 null mice show vast hypocellularity in the posterior pituitary gland. Here, POU3f2 is expressed primarily in neurons which are responsible for oxytocin and corticotropin releasing hormone (CRH) expression[74,95,76]. POU3f2 expression in combination with Asc1l, and Myt1l has been shown to convert fibroblast into neurons, astrocytes and oligodendrocytes[96].

1.2.5 POU3f2 in tumor development

POU3f2 is aberrantly expressed in several malignancies, such as melanoma[68], small cell lung carcinoma[97], neuroblastoma, merkel cell carcinoma and glioblastoma[70]. Moreover, based on The Human Protein Atlas Database, POU3f2 is expressed in cancer cell lines from various cancer types[98]. Publications concerning POU3f2 are rare; most research has investigated POU3f2 on melanomas[68,69,70], additionally nobody has yet systematically considered POU3f2 expression patterns in human gliomas albeit little data is available for the expression of POU3f2 in normal brains[99,88] and in brain tumors[100].

In normal tissue, differentiation of immature melanoblasts into pigmented melanocytes is associated with downregulation of POU3f2, while dedifferentiation of fully mature melanocytes to non-pigmented melanoblasts is correlated with an increase of POU3f2[69]. Notably, POU3f2 expression in melanomas is much higher than in primary melanocytes[69,70]. Upregulation of POU3f2 and is associated with proliferation and invasion[101] suggesting that

this upregulation is a critical step in melanoma progression[70]. Retinoblastoma (Rb) cells and small cell lung cancers are other tumors displaying POU3f2 expression. In both the Rb is typically mutated suggesting a link between dysregulated POU3f2 expression and retinoblastoma tumorgenesis[102].

2. Aims

2.1 Hypothesis

CNS neuronal and glial cell types share a common neuroectodermal origin with melanocytes. Moreover, the fetal transcription POU3f2 is highly expressed during neuronal development and in immature melanoblasts. Thus, it is possible that tumors arising from these tissues also display similarities. Since several studies have shown that POU3f2 is expressed at high levels in melanomas, we therefore hypothesized that POU3f2 is expressed in human gliomas.

2.2 Aims

1. To investigate the expression of POU3f2 in human glioma biopsies.
2. To investigate how POU3f2 impacts on proliferation and colony formation in genetically modified U251 glioma cells with overexpression and knock down for the POU3f2 gene.
3. To investigate how POU3f2 impacts on tumor growth *in vivo* by xenografting the above mentioned glioma cell line in mice.

3. Materials

Table 3.1: Software

Software	Supplier
Microsoft Office	Microsoft Corporation, Washington, USA
Adobe Photoshop	Adobe Systems Inc, CA, USA
Image J	NIH, Maryland, USA
Light Cycler 480 SW	Roche Applied Science, Germany

Table 3.2: Cell lines

Cell lines	Source	Distributor
293T Cells	Humman embryonic kidney cells	ATCC, Manassas, Virginia, USA
U251 MG	Humman glioblastoma, astrocytoma	ATCC, Manassas, Virginia, USA

Table 3.3: Primary Antibodies for ICC, IHC and Western blot

Protein	Source species and clonality	Dilution	Supplier	Cat number
Pou3f2	Rabbit, Polyclonal IgG	1:500/WB, 1:100/ICC, 1:100/IHC	Cell Signalling, Danvers, Massachusetts, USA	12137s
Pou3f2	Rabbit, Polyclonal IgG	1:200/IHC	Santa Cruz Biotechnology, California, USA	SC-28594
Pou3f2	Mouse, Monoclonal, IgG	1:500/IHC	Merck Millipore, Billerica, Massachusetts,USA	Q1980077
Pou3f2	Rabbit, Polyclonal, IgG	1:200/IHC	Lifesapan Biosciences, Seattle, Washington, USA	Ls-B7993
Pou3f2	Rabbit, Polyclonal, IgG	1:500/IHC	Proteintech, Chicago, Illinois , USA	18998-1-AP
GAPDH	Rabbit, Polyclonal, IgG	1:2000/WB	Abcam, Cambridge, United Kingdom	ab9485
WB: Western blot, ICC: Immunocytochemistry, IHC: Immunohistochemistry				

Table 3.4: Secondary Antibodies

Secondary Antibody	Source species	Dilution	Supplier	Cat number
HRP	Goat Anti-Rabbit IgG	1:20000/WB	Beckman Coulter, Marseille, France	IM0831
HRP	BIOTINYLATED Goat Anti-Rabbit IgG	1:100/IHC	Vector, Burlingame, California, USA	BA-1000
HRP	BIOTINYLATED Hourse Anti-Mouse IgG	1:100/IHC	Vector, Burlingame, California, USA	BA-2001
Florochrome	Goat Anti-Rabbit,IgG1, Human, TXRD	1:200/ICC	Southern Biotech, Birmingham, Alabama,USA	4010-05

Table 3.5: Primers for qRT-PCR

Target gene	Primer sequence
Pou3f2	Fw 5´- AGCAGTTCGCCAAGCAATTC-3´
Pou3f2	Rev 5´- CGAGAACACGTTGCCGTACA-3´
18S	Fw 5´- CGGCTACCACATCCAAGGAA-3´
18S	Rev 5- GCTGGAATTACCGCGGCT-3´

4. Methods

4.1 Cell handling

4.1.1 Cell culture

All work areas and equipment were disinfected with 70% ethanol and all cell handling procedures were done under a laminar flow hood (NUAIRE, Plymouth, Minnesota, USA). The cells were maintained in tissue culture incubators (SANYO Electric Co.Ltd, Moriguchi City, Osaka, Japan) at 37 °C with 5% CO_2, 100% humidity and 95% air. Depending on the number of cells that were needed for experiments, three different sizes (25 cm^2, 75cm^2 and 175cm^2) of culture flask (Nunc, Thermo Fischer Scientific, Waltham, kamstrupvej90, Denmark) were used for cell culturing. The adherent cells were cultivated as monolayers to 80-90% confluency in Dulbeccos Modified Eagles Medium (DMEM-ALT (DMEM supplemented w. 10% heat inactivated calf serum, four times the prescribed amount of non-essential amino acids, L-Glutamine, penicillin (100 μg/ml) and streptomycin (100 μg/ml)) (Sigma Aldrich, St. Louis, Missouri, USA). To passage cells, the old medium was removed and cells were washed twice with 1X PBS (phosphate buffered saline) (Sigma Aldrich, St. Louis, Missouri, USA). Then, the cells were detached by incubation at 37ºC in Trypsin-EDTA (Lonza, Basel, Switzerland) for 3-5 minutes. The effect of the trypsin was deactivated by adding DMEM-ALT. About 80% of the cells were discarded, and fresh DMEM-ALT was added. The passage number was registered each time that cells were passaged.

4.1.2 Cryopreservation of cells

Cells were frozen down for cryopreservation at the first passaging of newly thawed cells, for later use. For cryopreservation, cells were harvested when they were approximately 80% confluent. Trypsinization was performed as previously explained and approximately $1{,}8X10^7$ cells were transferred into a 15 ml centrifuge tube (Thermo Scientific Nunc, Rochester, USA) and centrifuged at 900g for 5 minutes. Supernatant was discarded and pelleted cells were resuspended in 8 ml of freezing solution (1 ml DMSO (Sigma-Aldrich, St. Louis, Missouri, USA), 1 ml 10% FBS (Invitrogen, Carlsbad, California, USA) and 6 ml medium). The suspensions were aliquated into 8 cryotubes (1 ml each) (Nunc, Thermo Fischer Scientific, Waltham, Massachusetts, USA) and placed in an isopropanol container in -80ºC

freezer overnight. After 24 hours the cryotubes were transferred to a liquid nitrogen tank maintained.

4.1.3 Thawing of cells

Cells were thawed at 37°C in a water-bath. Thereafter, the cell suspension (1 ml) was transferred to a 25 mm^2 flask containing 10 ml DMEM-ALT. The medium was replaced with 10 ml of fresh medium after 24 hours.

4.1.4 Counting of the cells

Depending on the type of the experiments, cells were counted before, during or after the experiment, using a Burker chamber (hemocytometer or counting chamber) (Marienfeld-Superior, Lauda-Königshofen, Germany). Burker chambers contain a big central square with 9 squares, and each of these 9 squares encloses 16 smaller squares. The numbers of cells were counted in 3 of 9 squares and divided by three to achieve the average number of cells per square. This number was multiplied by 10^4 to estimate the number of the cells per milliliter. An inverted light microscope was used for cell counting and cell monitoring.

4.2 Cryostat tissue sectioning

A cryostat (Leica CM 3050S Cryostat, Nussloch, Germany) was used to prepare cryosections to extract DNA, RNA and protein. Sectioning performed at -20 ºC. All the necessary equipment was placed in the cryostat chamber before using. The tissue samples were taken from nitrogen tank and the temperature was increased to -20ºC and then embedded into an optimal cutting temperature compound (O.C.T) (Sakura Finetek, Torrance, California, USA) and sectioned to a 10-12 µm. About 40-60 of the sections (depending on the size of the samples) were collected for DNA, RNA and protein extraction (the samples were stored at -80ºC until using). Control sections were inspected microscopically to confirm that they contained tumor tissue.

4.3 Hematoxylin and Eosin (H&E) Staining

Prepared slides from the cryostat were immersed in 50% ethanol/methanol (Sigma-Aldrich, St. Louis, Missouri, USA) for 5 minutes and dried at room temperature for 10 minutes. Thereafter, the slides were stained for 1 minute by hematoxylin (Cellpath, Newtown, Powys,

UK) and were washed in running tap water until the water was clear. The sections were stained with eosin (1gram eosin, 20 ml distilled water, 180 ml 96% ethanol) for 20 seconds and the excess eosin was rinsed away in several changes of tap water. Sections were dehydrated in 96% ethanol (2 minutes) and 100% ethanol (2 minutes), and then placed in Xylol (Sigma-Aldrich, St. Louis, Missouri, USA) for 4 minutes. Finally, a glass coverslip was mounted on Entellan (Merck, Darmstadt, Germany) on top of the sections.

4.4 Immunohistochemistry

4.4.1 Immunohistochemistry

In this study the Avidin-Biotin complex (ABC) method was used on samples of formalin fixed paraffin embedded tissue sections. Briefly, this method uses a biotinylated secondary antibody and subsequent addition of an avidin-biotin complex (ABC reagent)[103].

4.4.2 Deparaffinising and dehydration

The slides were dipped in Xylol twice (Sigma Aldrich, St. Louis, Missouri, USA) 5 minutes each time, transferred to absolute ethanol twice, and then 96% ethanol twice, 3 minutes for each wash. Finally, slides were immersed in Milli-Q water for 2 minutes.

4.4.3 Antigen retrieval

Heat induced epitope retrieval (HIER) was used for antigen retrieving[104]. The slides were placed in boiling citrate buffer (pH 6) and incubated in a 98°C water bath (IKA-WERKE, Germany) for 20 minutes. The container was cooled down at room temperature (RT) for 15 minutes and subsequently then kept in running water for 10 minutes. The tissue sections were encircled with a water-repellant hydrophobic barrier pen (ImmEdge pen, Burlingame, California, USA). Thereafter, TBS w/Tween (0.05M Tris, pH 7.2-7.6, 0.3 M NaCl, 0.1% Tween 20 (Sigma Aldrich, St. Louis, Missouri, USA)) was added on each section and the slides were then washed by TBS w/Tween two times for 3 minutes.

4.4.4 Blocking and antibody treatment

TBS w/Tween was sucked up and replaced by a blocking buffer (Bovine Serum Albumin (BSA)) (5 mg/ml) (Sigma Aldrich, St. Louis, Missouri, USA) and incubated for 30 minutes at RT. Next, the primary antibody (Table 3.3) was diluted in the blocking buffer, added to

the sections and incubated for 1 hour at RT or incubated overnight at 4°C in a humidified chamber (depending on the antibody). Then slides washed by TBS w/Tween 3x3 minutes. hydrogen peroxide (hydrogen peroxide (30 µl/ml) was diluted in 1X PBS) and added for 5 minutes at RT, and washed by TBS w/Tween three times for 3 minutes each. Thereafter, a biotin-conjugated secondary antibody (Table 3.4) was diluted in the blocking buffer and added to the sections for 1 hour at RT, before slides were washed as described in earlier steps. The Avidin-biotin complex (ABC Reagent) (Vector Laboratories Inc., Burlingame, California, USA) was added for 30 minutes at RT. After washing three times with TBS w/Tween washing buffer, 100 µl of DAB substrate-chromogen (1 drop of 3,3'-diaminobenzidine in chromogen solution + 1ml of Imidazole-HCl buffer, pH 7.5, containing hydrogen peroxide and an anti-microbial agent) (Dako, Carpinteria, California, USA) was added to the sections for varying time durations (30 second to 7 minutes). Then the sections were washed by Milli-Q water first and then immersed in Milli-Q water until next step. The substrate reaction was monitored through a light microscope. For negative control just secondary antibody was added to the samples.

4.4.5 Counterstaining and dehydration

The slides were dipped in hematoxylin (filtered before use) for 60-90 seconds and washed in running tap water. The sections were dehydrated by dipping the slides in different percentages of ethanol and absolute xylene as follows: distilled water 2 minutes, 96% ethanol 2x3 minutes, absolute ethanol 2x3 minutes and xylene 2x5 minutes.

4.4.6 Mounting

Entellan (xylene-base mounting medium) was added on xylene-wet sections and then a coverslip was mounted on top. The light microscope was used for analyzing the sections.

4.4.7 Percentage Calculation for expression of interest protein

The POU3f2 staining was predominantly nculear which allowed us to estimate the nuclear labelling index as the fraction of immunopositive nuclei compared to all (immunopositive and negative nuclei). Each image was divided into 16 parts and 3 out of the 16 grids for each sample (the grid pattern was same for all the samples) were assessed at 200x magnification.

4.4.8 Optimization

Five antibodies (against POU3f2) from different companies (Millipore Corporation, Cell Signaling Technology, Santa Cruz Biotechnology, Life Span Technologies, Protein Tech Group) were tested, and optimized for both dilution (1:100, 1:200, 1:500, 1:1000) and incubation time (1 hour or overnight).

4.5 Immunocytochemistry

4.5.1 Immunocytochemistry

In this study, we used an indirect method[105] for detecting cellular protein with a secondary antibody conjugated to a fluorescent tag – a fluorophore.

4.5.2 Sample preparation

Sterile 12 mm coverslips were placed in a 24-well plate and 20000-40000 cells were seeded on each coverslip. The amount of DMEM-ALT was increased to 1 ml in each well and the cells were maintained in tissue culture incubators at 37ºC with 5% CO_2, 100% humidity and 95% air. At 70-80% confluency, the cells were washed 2 times with 1X PBS after removing the old media. To fix the cells, about 500 µl of paraformaldehyde (40 mg/ml, diluted in 1X PBS) (Thermo scientific, Rockford, Illinois, USA) was added to each well and incubated for 10 minutes at room temperature. Next, the paraformaldehyde was removed and 500 µl of Triton X-100 (5 µl/ml, diluted in 1x PBS) (Sigma Aldrich, St. Louis, Missouri, USA)) was added to each well for 4 minutes to permeabilize the cells. After removing the Triton X-100, the cells were washed with 1X PBS 3 times and stored in 1X PBS at 4 ºC.

4.5.3 Immunostaining

A humidified box covered with parafilm used for the procedure. The cells were blocked by bovine serum albumin (BSA) (5mg/ml, diluted in 1x PBS) (Sigma Aldrich, St. Louis, Missouri, USA) for 15 minutes at RT. Subsequently, cells were incubated with the primary antibody (diluted in BSA (5mg/ml) in 1x PBS) (Table 3.3) overnight at 4 ºC. Then, cells were washed for 3x3 minutes with 1X PBS and then incubated with the secondary antibody (diluted in BSA (5mg/ml) in 1X PBS) (Table 3.4) for 45 minutes at 37℃. Afterwards, cells were washed with 1X PBS for 3x3 minutes. Subsequent steps were conducted with the lights off. 5 µl Prolong Gold (mounting solution) antifade reagent containing 4',6-diamidino-2-

phenylindole (DAPI) (Invitrogen, Eugene, Oregon, USA) was added to the glass slides, before the coverslips were mounted on the sections. The mounting solution was allowed to dry overnight. For negative control, the primary antibody was omitted from the procedure.

4.5.4 Fluorescence imaging

The Nikon TE2000 inverted microscope (Nikon instrument, Inc. Tokyo, Japan) was used to examine the ICC samples. This microscope is equipped with a mercury arc lamp, and a set of fluorescence filters ranging from UV to far red. Bandpass filters were used to capture the different required wavelengths.

4.6 Protein immunoblotting

4.6.1 Immunoblotting

Immunoblotting (Western blotting (WB)) is used to detect a protein of interest in a protein mixture. In immunoblotting the proteins are generally sorted by molecular weight and the separated protein bands are then transferred to a membrane. The membrane is incubated with primary and secondary antibodies for the stipulated duration of time. Subsequently, antibodies bind to the interest protein and make the protein band visible[106].

4.6.2 Protein isolation

Proteins were extracted from cells or brain tumor tissue. To extract proteins from the cells, they were seeded in a 25 mm^2 flask and incubated at 37°C with 5% CO_2, until the cells reached 80-90% confluency. Then, media was removed and the cells were washed with cold 1X PBS twice. While the flask was placed on ice, 200 µl Kinexus protein lysis buffer (500 mM MOPS, 500 mM EDTA, 100 mM EGTA, 500 mM NaF, 10% Triton X, 100 mM PMSF ((in isopropanol), pH 7.2), protease inhibitor cocktail tablet (Roche, Mannheim, Germany) and phosphatase inhibitors cocktail tablets (Roche, Mannheim, Germany) (each 10 ml of Kinesus protein lysis buffer contained 1 tablet of protease and phosphatase inhibitor) were added to the cells and after 5 minutes incubation on ice, the cells were collected by cell scrapers and transferred to a 1,5 eppendorf tube and incubated on ice again for 5 minutes. For more disruption of the cell membranes, a sonicator (Sonics Vibra-Cell, Illinois, USA) was used at 20 Hz for 3x2 seconds. Samples were centrifuged at 13200 for 30 minutes at 4 ºC. The supernatant was transferred to a new 1.5 ml eppendorf tube and stored

at -20 °C. To extract the brain tumor tissue, 200 µl Kinexus protein lysis buffer was added to the tissue sections, which had been homogenized using a small pestle (the pestle was changed sample by sample). After homogenization, tissue samples were sonicated and centrifuged; the supernatant was stored in the same way the cell lines.

4.6.3 Measurement of protein concentration

The protein concentration was measured using NanoDrop 1000 Spectrophotometer (Thermo Fisher Scientific). Based on the nanodrop manual 2 µl of Kinexus protein lysis buffer was added to the lower measurement pedestal of nanodrop as a blank and then 2 µl of each protein sample was loaded for measurement[107]. After each measurement, the lower and upper pedestals were wiped by a soft laboratory wiper and then the next sample was loaded for concentration measurement. Nanodrop is able to detect absorbance wavelengths between 220-750 nm and it measures the protein absorbance at 280 nm and calculates the concentration in mg/ml.

4.6.4 Sample preparation and SDS-PAGE

To prepare the sample for SDS-PAGE gel electrophoresis, 10-40 µg of protein was mixed with 2.5 µl of reducing agent (Invitrogen, Carlsbad, California, USA), 7.5 µl of 4X LDS sample buffer (Invitrogen) and distilled water (dH2O) was added until the total volume reached 30 µl. The samples were boiled for 10 minutes at 70°C and then briefly centrifuged (10000 g for 30 seconds). A 10-well NuPage (1.5 mm) 4-12% Bis-Tris gel (Invitrogen) was assembled using a Novex mini-cell gel chamber (Invitrogen), the inner chamber was filled with 200 ml 1X NuPage MES Running Buffer (Invitrogen) including 500 µl of antioxidant (Invitrogen) and the outer chamber was filled with 600 ml of 1X running buffer. To remove any air bubbles, wells of the gel were flushed with running buffer before loading. Subsequently, 5 µl of SeeBlue plus 2 Prestained Standard (Invitrogen) were loaded to the gel as molecular weight standard and 30 µl of each sample mixture was loaded next to the molecular weight standard. The mini-cell gel chamber was placed onto ice and the electrophoresis was run at 140 V for 85 min.

4.6.5 Blotting

Separation of proteins on the SDS-PAGE is required before transfer onto a nitrocellulose membrane (blotting). Electrical current was used to transfer protein from the SDS-PAGE to the nitrocellulose membrane. Three blotting pads, one filter paper, the SDS-Gel, 0.2 µm

nitrocellulose membrane (Whatman International Ltd., Kent, UK), one filterpaper and three blotting pads again were assembled in an XCell II Blot Module from cathode to anode respectively and fixed in a Novex mini-cell gel chamber. The transfer chamber was filled with transfer buffer (25 ml 20X transfer buffer (Invitrogen), 50 ml methanol and 500 µl antioxidant (Invitrogen) were filled up to 500 ml with MilliQ-water) and the outer chamber was filled with MilliQ-water. Finally, the Novex mini-cell gel chamber was placed on the ice and transferring was run at 30 V for 80 minutes. Before assembling, all the components except the gel were soaked in the prepared transfer buffer; moreover, a roller was used to expel air bubbles between the layers.

4.6.6 Ponceau S staining

After blotting, the nitrocellulose membrane was washed in MilliQ-water and was then incubated in Ponceau S dye (0.1% ponceau S dye in 5% acetic acid) for 10 minutes at room temperature to verify the efficiency of the transferring. Thereafter, the membrane was washed with MilliQ-water to remove any excess dye. For further analysis, the membrane was scanned after staining. Finally, the membrane was cut based on the molecular weight of the target protein and used for blocking and for subsequent steps.

4.6.7 Blocking and antibody incubation

In order to block unspecific binding, a nitrocellulose membrane was incubated in blocking buffer (Difco Skim Milk Powder (50 mg/ml)) diluted in 1X TBS w/Tween) (BD Biosciences, Franklin, Lakes, New Jersey, USA) for 1 hour at RT while gently shaking. The primary and secondary antibodies were diluted in blocking buffer (Table 3.3 and table 3.4). Thereafter, the membrane was incubated with the primary antibody at 4°C overnight. Next, the membrane was washed with TBS w/Tween (20 ml 0.5 M Tris/HCl pH 7.5, 75 ml 1M NaCl, 0.5 ml Tween 20, Adjusted to 500 ml with MilliQ H2O) for 4x10 minutes at RT. After that, the membrane was incubated with the secondary antibody (Table 3.4) for 90 minutes at RT and was then washed using TBS w/Tween for 4x10 minutes. The incubation and washing step were done on the shaking board. The housekeeping gene GAPDH (Glyceraldehyde-3-phosphate-dehydrogenase) was used as an internal control to check the quantity of the loaded protein for each patient (Table 3.3).

4.6.8 Chemiluminescence and quantification of protein expression

In order to visualize the protein-antibody interaction, a membrane was incubated with Super Signal West Femto Maximum Sensitivity Substrate (Thermo Fisher Scientific, Waltham, Massachusetts, USA) for 5 minutes at RT. Super Signal West Femto Substrate with horseradish peroxidase (HRP) enzyme used for immunoblotting. The luminescent image analyzer LAS-3000 (Fujifilm Medical Systems Inc., Stamford, Connecticut, USA) was used for imaging. Finally, the relative proteins expression levels were quantified using Image J software (NIH, Maryland, USA) based on the software's guidelines[108]. In this procedure, the band density of each protein was normalized with the band density of the GAPDH for the same patient. Subsequently, the relative density was calculated for all the samples.

4.6.9 Optimization

To determine the optimal protein concentration the western blot experiment, different concentrations (10-50 µg) of the protein mixtures (human gliomas samples) were loaded on the gel. Based on this procedure we decided to load 40 µg of protein from each sample.

4.7 Quantitative Real Time Polymerase Chain Reaction (qRT-PCR)

4.7.1 qRT-PCR

Quantitative Real Time Polymerase Chain Reaction (qRT-PCR) is a technique used to amplify and quantify a DNA sequence of interst[109]. qRT-PCR is based on the polymerase chain reaction (PCR) in which a quantity of the interest sequence is detected by fluorescent dye; the fluorescent dye can intercalate to the double strand DNA non-specifically or it can bind to the specific sequence of the DNA[109]. In this study, Non-specific DNA binding dye was used as a fluorescent reporter to determine the amount of the gene expression.

4.7.2 RNA isolation

RNA was isolated from cells and tissue samples using Qiagen RNeasy Mini kit (Qiagen, Hilden, Germany) according to the manufacturer's instructions[110]. 20-30 mg of tissue was collected by a cryostat (according to section 4.2). To isolate RNA from the cells, cells were treated by trypsin-EDTA as explained in Section 4.1.1. The trypsin was inactivated by adding 5 ml DMEM-ALT. Next, the cells were centrifuged for 5 minutes at 900 g after transferring to a 15 ml tube. The cell pellet was resuspended in 1X PBS and centrifuged at

900 g for 5 minutes. The supernatant was removed and the pellet was collected for RNA extraction. According to the manufacture's instruction up to ~10^7 cells were used.

4.7.3 Removal of DNA from RNA

The RNase-Free DNase Set (Qiagen, Hilden, Germany) was used to remove residual DNA contamination from the RNA samples. 10 µl of DNase I stock solution was added to 70 µl of Buffer RDD for each RNA sample and mixed gently. Next, 80 µl of mixed solution was added to the RNease spin column membrane while RNA was bound to the RNeasy membrane and incubated for 15 minutes at RT.

4.7.4 Measurement of RNA concentration and quality determination

Agarose gel electrophoresis is a technique used to separate nucleic acids by size. The nucleic acids can migrate in the agarose gel due to the negative charge of the phosphate in the back bone of the nucleic acids[111]. The agarose gel electrophoresis was performed to evaluate the quality of the extracted RNA. 3 µl of RNA was mixed with 3 µl of 2x RNA loading dye (Thermo Fisher Scientific, Waltham, Massachusetts, USA) and 5 µl of the mixture was loaded on to 1% agarose gel (10 mg/ml in 1X Tris-Acetate-EDTA (TAE) buffer (40 mM Tris base, 2 mM EDTA, Acetic acid 20 mM, Adjust to pH 8.5 and dilute to 1X with Milli-Q H_2O before use)) containing 3 µl of ethidium bromide (10 mg/ml) (Sigma Aldrich, St. Louis, Missouri, USA). The gel run for 30 minutes at 100 V. Finally, a UV-imager (Fujifilm Medical Systems Inc., Stamford, Connecticut, USA) was used to scan the gel. The RNA concentration was measured by a NanoDrop1000 Spectrophotometer (Thermo Fisher Scientific). Based on manual instruction, 1 µl of RNA was loaded to the lower measurement pedestal and Nuclease free water was used as a blank. The Nanodrop measures the Nucleic acid absorbance at 260 nm and calculates the concentration in ng/µl[107].

4.7.5 cDNA synthesis and determination of cDNA concentration

Making complementary DNA (cDNA) from RNA is a necessary process for performing quantitative qRT-PCR. The iScriptc DNA Synthesis kit (BIO-RAD, Hercules, California, USA) was used for making cDNA from RNA. To make cDNA, according to the manufacturer's instructions 4 µl of 5X iscript mix, 1 µl of iscript reverse transcriptase, x µl of Nuclease-free water and x µl of RNA template (250 ng RNA was used for each sample) were mixed to a total volume of 20 µl. The mixture was incubated for 5 minutes at 25°C, 30

minutes at 42°C and 5 minutes at 85°C by using a Peltier Thermal Cycle (BIO-RAD, Massachusetts, USA). Finally, the cDNA was diluted 10 times and stored at -20ºC.

4.7.6 Plate preparation, running and analysis

The iQ SYBR Green Supermix kit (BIO-RAD, USA) was used to perform qRT-PCR. For one reaction, 5 µl of iQ SYBR Green Supermix, 2 µl of 1 µM primer pairs (Table 3.5), 1 µl of Nuclease-free water and 2 µl of cDNA were loaded on a 384 well plate. Each sample was loaded in triplicates and each plate was run three times on a Roche LC480 instrument (Roche Applied Science, Germany). The resultant qRT-PCR program was used to perform thermal cycles: Initial denaturation 95 ˚C – 5 min, denaturation 95 ˚C – 10 sec, annealing 60 ˚C - 10 sec, extension 72 ˚C – 10 sec, final extension 72 ˚C - 5 min and finally, held in 4 ˚C. Non-Template Control (primer was added to master mix without any cDNA) was run to check the possibility of dimer formation and non-specific amplification. In all qRT-PCR experiment, the eukaryotic ribosomal gene 18S was used as a control (Table 3.5).

Finally, the ΔΔCT method was used to calculate fold change of the gene expression[109].

4.8 Lentiviral Transduction

4.8.1 Transformation

The lentiviral constructs (pLenti-POU3f2-GFP (Hereafter called “POU3f2 ox”) and pLenti-GFP (Hereafter called “blank vector”), pLenti-POU3f2-siRNA-GFP (Hereafter called “POU3f2 siRNA”) and pLenti-Scrambled siRNA-GFP (Hereafter called “scrambled siRNA”)) were bought commercially from Applied Biological Materials, Canada. To amplify these plasmids, a heat shock method was used to transform the plasmid of interest to the bacteria[112]. The NEB10-beta competent *Escherichia coli* (*E. coli*) (New England Biolabs, MA, USA) were thawed on ice and 10 ng of plasmid DNA was added to 30 µl of the cells. The cells and plasmid were mixed by gentle flicking in the microcentrifuge tube. The tube was incubated on ice for 20 minutes and heat shock was performed by placing the microcentrifuge tube into a 42˚C water bath for 45 seconds. Thereafter, the tube was placed on ice for 5 minutes. After 5 minutes of incubation on ice, 450 µl of prewarmed Super Optimal broth with Catabolite repression medium (SOC medium) was added to the mixture and incubated for 1 hour at 37ºC in a shaking incubator at 200 rpm. Subsequently, 100 µl of transformed bacteria was added to Lysogeny broth agar (LB agar plate) (Tryptone (1

mg/ml), yeast extract (0.5 mg/ml), Nacl (1 mg/ml) in 1 liter H2O, pH adjusted to 7.0 with 5 N NaOH, 15 mg/ml agar dissolved in 1 liter of LB medium) containing 50 µg/µl kanamycin and the bacteria suspension was spread using a sterile glass spreader. The plates were left about 10 minutes before incubation at 37 °C overnight.

4.8.2 Plasmid purification

One of the transformed bacterial colonies was taken and added to 20 ml of LB medium containing kanamycin (50µg/ml) and incubated overnight at 37°C while shaking at 200 rpm. Next day, 19 ml of the bacteria were transferred to a new tube and the tube was centrifuged for 30 minutes at 4000 rpm. Supernatant was removed and the pellet was used for plasmid purification. E.Z.N.A.® Plasmid DNA Mini Kit II (Omega bio-tek, Georgia, USA) was used to purify plasmid DNA according to the manufacturer's instructions.

4.8.3 Restriction digestion

Plasmids were digested by a restriction enzyme and agarose gel electrophoresis was performed to confirm the identity of the plasmids. Digestion of the plasmids was performed by preparation of a 10 µl mixture including 1 µl DNA, 0.5 µl Enzyme (PstI (pLenti-POU3f2-GFP and pLenti-GFP), SmaI (pLenti-POU3f2 siRNA-GFP and pLenti-Scrambled siRNA-GFP)) (Promega, Wisconsin, USA), 1 µl 10X buffer, 0.1 µl BSA and 7.4 µl of water. The mixture was incubated at optimum temperature of the enzyme (SmaI: 25ºC and PstI: 37ºC) for two hours. Thereafter, samples were electrophoresed through 1% agarose gel (10 mg/ml in 1X TAE buffer) containing 3 µl of ethidium bromide. 6 µl of DNA was mixed with 1µl of loading dye (6X) (Thermo Scientific Nunc, Rochester, USA), and 5µl of 1KB DNA marker standard (Thermo Scientific) was loaded to the first well. The gel run at 100V for 25 minutes.

4.8.4 Lentivirus production: $CaPO_4$ transfection

For virus production, 1.6×10^6 293T cells were seeded in a small flask and incubated at 37ºC with 5% CO_2 overnight until the cells reached 70-80% confluency. The next day, the medium was replaced with an 8ml low Pen/Strep medium containing DMEM (42.9 ml), pen/strep (100 µl), glutamine (1 ml), non-essential amino acid (1 ml) and FBS (5 ml). Next, 528 µl of BES-buffered saline 2X (BBS) was added in drops to the mixture of plasmids including 106 µl of Cacl2 (2M), GagPol Rev (M334) (1130 ng), Env (M5) (268 ng), lentiviral vector (4178 ng) and 422 µl of dH2O and mixed well by pipetting up and down.

After 15 minutes of incubation at RT, 1054 µl of the mixture was added drop by drop to flasks containing 293T cells and incubated at 37ºC with 3% CO_2. The next day, transfection efficiency was evaluated by fluorescent microscopy in order to check the presence of GFP in lentiviral plasmids. Thereafter, the medium was replaced with fresh DMEM-ALT and the virus was collected during at the next two days. Viruses were filtered by a 0.2 µm filter (Acrodisc Syringe Filter, Pall Life Sciences, USA) and stored at -80°C.

4.8.5 Lentiviral infection

For cell infection, 4×10^4 cells were seeded in a 24 well plate, and cells were incubated overnight at 37ºC with 5% CO_2. The next day, a different dilution of viruses (100, 200, 300 µl) with 1µl of polybrene (5mg/ml) was added to each well (different wells with the same cell lines). Plates were centrifuged at 2250 rpm for 90 min at 3ºC and then incubated at 37ºC with 5% CO_2. After successful transfection, positive cells were selected with puromycin, and were sorted by FACS (fluorescence activated cell sorting). This step was performed by a collaborator. The positive cells were cultured and used for planned experiments.

4.9 Proliferation assay

Growth curves were established to characterize cell proliferation for different cell lines. 15000 cells were seeded in each of three small flasks and the flasks were kept at 37ºC with 5% CO_2. The number of cells in each flask was counted every third day until day 12 (day 3, 6, 9 and 12). To count the cells, they were trypsinized (Section 4.1.1) and 10 µl of cell suspension was loaded into a Burker chamber (Section 4.1.4). The average number of the cells in the three flasks was used to determine the growth curve. The proliferation assay was performed two times.

4.10 Clonogenic assay

To perform clonogenic assay, 500 cells were seeded into a six-well plate and then the plates were incubated in a normoxic incubator for 10 days. At day 10, the medium was removed, and wells were washed with 1X PBS. Thereafter, to fix the cells, 500 µl of paraformaldehyde (40 mg/ml, diluted in 1X PBS) was added to each well and left for 5 minutes. After fixation, the paraformaldehyde was removed, and crystal violet solution was added to the wells for 15

minutes. Finally, the wells were washed with tap water and the plates were dried with air. The clonogenic assay was repeated there times.

4.11 Animal experiment

An *in vivo* animal experiment was performed to investigate the function of the POU3f2. In this experiment, U251MG (Hereafter called U251) cell lines (U251 POU3f2 ox, U251 POU3f2 siRNA and U251 scrambled siRNA) were implanted in intracerebrally in NOD-SCID mice. The mice were kept on a standard pellet diet, in a pathogen free environment at a constant temperature and humidity, on a standard 12/12 h light and dark cycle. The animals were provided a standard pellet diet and tap water ad libitum. Tumor formation was checked by a Positron emission tomography (PET) scan. This procedure involves the use of radioactive tracers and is therefore organised as a service platform, with specially trained personnel performing the experiments.

4.11.1 Animal welfare

Animal experiments were done in accordance with the Norwegian Animal Welfare regulations and all experimental procedures were approved by the Norwegian Animal Research Authority (Oslo, Norway).

4.11.2 Animal preparation and cell implantation

For anesthesia, the mice were kept in a chamber containing 5% isofluran until they became unconscious. The unconscious animals were then placed in Stereotactic frame (KOPF, Tujunga, California, USA) (Fig 4.11.2 A and Fig 4.11.2 B) while 2.5% isofluran was administered through a mask covering the nose and mouth of the mice. Before the operation, 0.5 ml Marcain (AstraZeneca, North Ryde NSW, Australia) was injected subcutaneously in the location of the surgery, and an incision was made on the scalp, (Fig 4.11.2 B). Then we found the point where Coronal Suture and Sagittal Suture meet, thereafter, from this point, we located 1.0 mm posterior to the coronal suture and 1.5 mm right of the midline (Fig 4.11.2 C). We drilled a hole in the marked location and entered the needle 2.5 mm below the cortical surface. 7.5×10^5 cells from each cell line (U251 POU3f2 ox, U251 POU3f2 siRNA and U251 scrambled siRNA) were injected into the mouse brain gradually (Fig 4.11.2 D). The skin was closed with 3 stitches. The mice were kept in an infant incubator until they became conscious; they were then transferred to the standard cage.

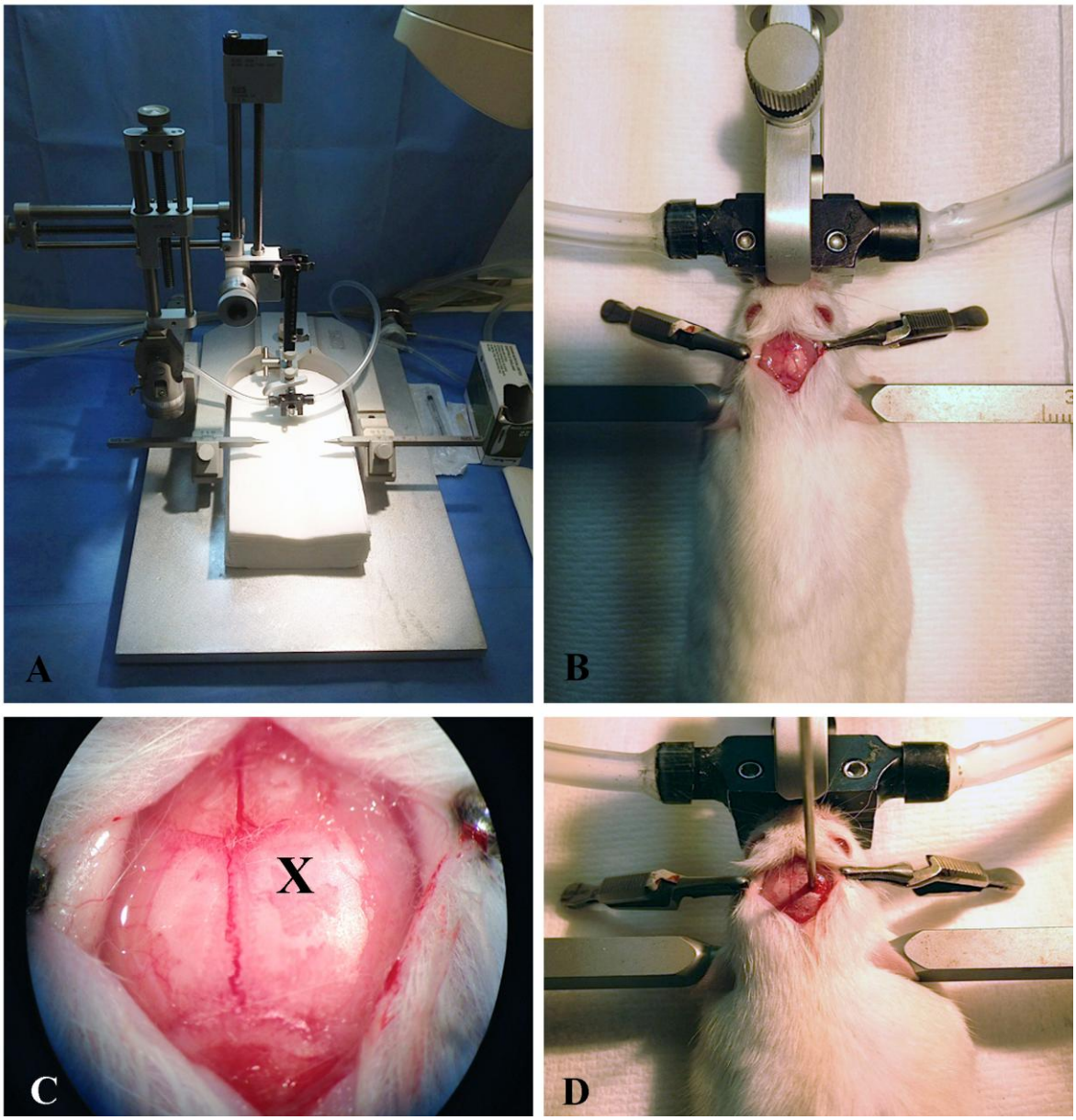

Figure 4.11.2 A. Stereotactic frame. **B.** A fixed mouse is shown in this figure. The mouse is held in position with nose and ear bars while 5% isofluran is streamed over mouse face. **C.** The approximate location of the injection is shown by X letter. **D.** 750000 cells were injected 2 cm deep into the mouse brain and the skin was closed by 3 stiches.

4.12 Statistical Analysis

Statistical analyses were conducted with the Graphpad Prism software version, 6.04 (Trial version). For the labeling indices on IHC, western blot and qPCR quantifications, gaussian distribution was assessed using the Shapiro-Wilk normality test. Neither band densities from western blots, labeling indices on IHC nor the qPCR values passed the normality test and we therefore used the non-parametric Kruskal-Walis to analyse the datasets from the three groups, followed by comparing the individual groups using Dunn's multiple comparison test. The results are presented as the average values± standard error of mean. Growth curves in the proliferation assay were compared using the Two-way ANOVA with repeated measures, followed by correction for multiple testing. Survival data were entered using the Kaplan-Meier survival plot, and the curves were compared using the logrank test. A p-value of ≤ 0.05 was considered significant.

5. Result

In this study, expression of POU3f2 was examined in a panel of approximately 40-50 human glioma biopsies (IHC=51 samples, WB= 37 samples and qRT-PCR=38 samples), and subsequently performed functional studies to establish how POU3f2 expression impacted on glioma cell growth *in vitro* and *in vivo*.

5.1 Investigation of POU3f2 expression in glioma patients by immunohistochemistry

In order to investigate the spatial distribution of POU3f2 expression in brain tumors, and its possible correlation with the malignancy grade, IHC was performed with 51 formalin fixed paraffin embedded patient biopsies from grade II-IV gliomas.

5.1.1 Evaluation of antibody specificity for POU3f2

In order to identify reliable antibodies against human POU3f2 for subsequent work, we obtained and validated five antibodies (against POU3f2) from different commercial providers (Section 4.4.8). Two samples series from two different GBM patients were stained with all 5 antibodies (anti-POU3f2) separately using their optimal dilution and incubation time (Fig 5.1.1). We found that all five antibodies gave a positive staining in paraffin sections against POU3f2. However, two of these antibodies (Life Span and Santa Cruz) stained almost complete sections with varying levels of intensity, suggesting unspecific binding (Fig 5.1.1). To assess POU3f2 expression in IHC sections, antibody from Millipore was selected for IHC experiment.

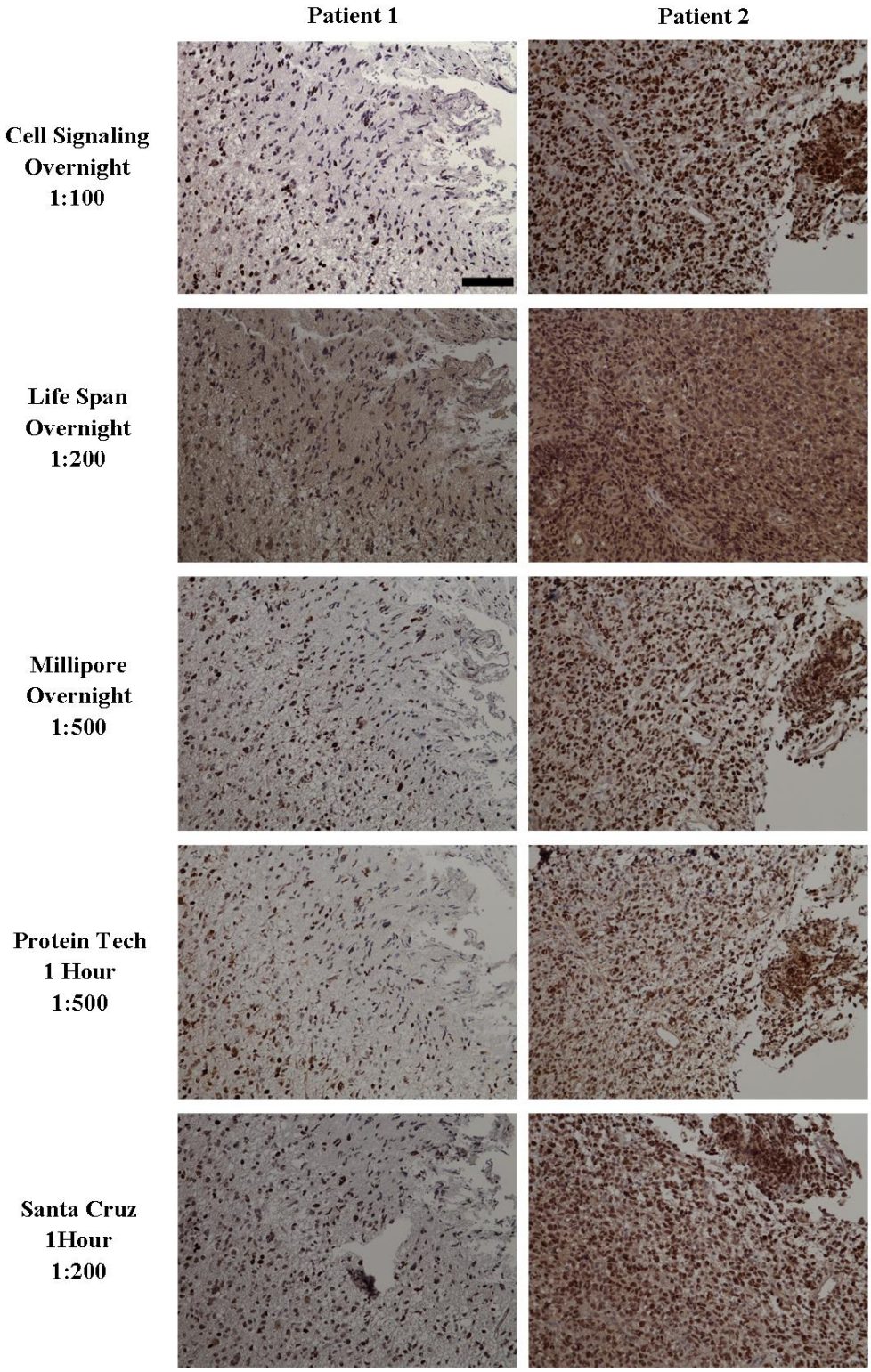

Figure 5.1.1 Antibody determination. Two randomly selected GBM patient samples were stained with 5 different antibodies (anti-POU3f2). The Avidin-Biotin immunohistochemistry method was used (Section 4.4) to stain formalin fixed paraffin embedded patient biopsies and then colorless substrate, DAB, was added. The Avidin-biotin enzyme complex converted the DAB substrate to a brown product. The brown color is shown to be POU3f2-positive cells. Moreover, counterstaining was done (Section 4.4.5) and resulted in the blue color of the POU3f2-negative cells. The magnification of the pictures is 20x and the scale bar = 100μm.

5.1.2 Evaluation of POU3f2 expression in glioma patients by Immunohistochemistry

Next, we conducted IHC with our validated antibody from Millipore to investigate the expression of POU3f2 in a larger panel of 51 biopsies from human gliomas (Fig. 5.1.2.b and appendix 9.1) of different grades: 11 grade II gliomas, 10 grade III gliomas and 30 grade IV gliomas (GBM). An expression of POU3f2 was detected in all samples of different grades (II, III, IV) while the rate of POU3f2 expression was highest in GBM and lowest in grade II. Expression of POU3f2 was predominantly observed in the nucleus of POU3f2-positive cells but also cytoplasmic expression was observed in some cells (FIG 5.1.2.a A), moreover, vessels also were stained by POU3f2 antibodies slightly (FIG 5.1.2.a B). Based on the nuclear POU3f2 expression, the POU3f2 nuclear labeling index (LI) was quantitated by two independent observers, through the visual inspection of randomly selected areas from all the tumor sections. The percentage of POU3f2 expression was 55.9% (+/- 4.2 SE) in grade II, 61.8% (+/- 5.1 SE) in grade III, 86.5% (+/- 1.9 SE) in grade IV. The representative average of POU3f2 expression in paraffin sections is shown in figure 5.1.2.b B. POU3f2 LI was significantly different between the groups (P-value = 0.0001, Kruskal-Wallis). Notably, the POU3f2 LI in grade IV gliomas was significantly higher than in grade II (P-value < 0.0001), and grade III (0.001>p>0.0001) gliomas. However, the POU3f2 LI for grade II and III gliomas was not significantly different.

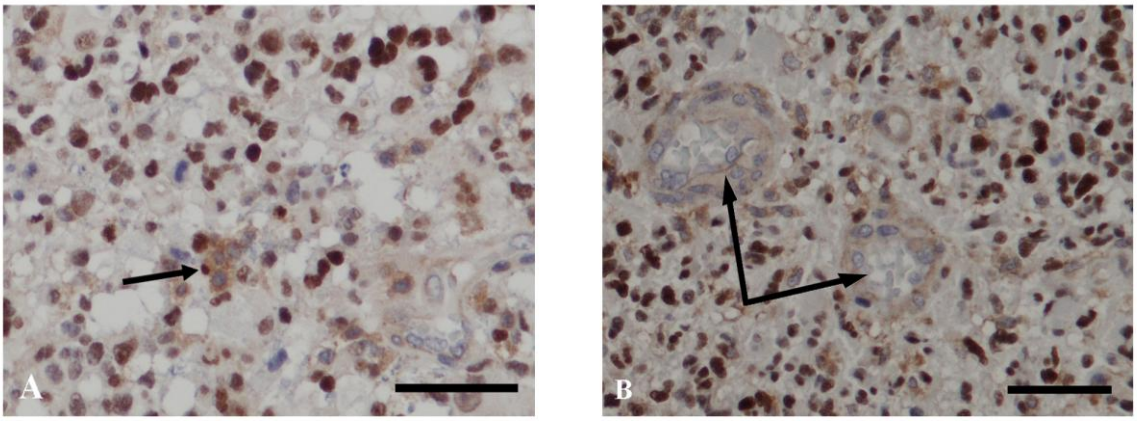

Figure 5.1.2.a POU3f2 staining of human glioma. **A.** Cytoplasmic expression of POU3f2. **B.** Staining of vessel by POU3f2 antibody. Magnification is 20x and scale bar = 50µm

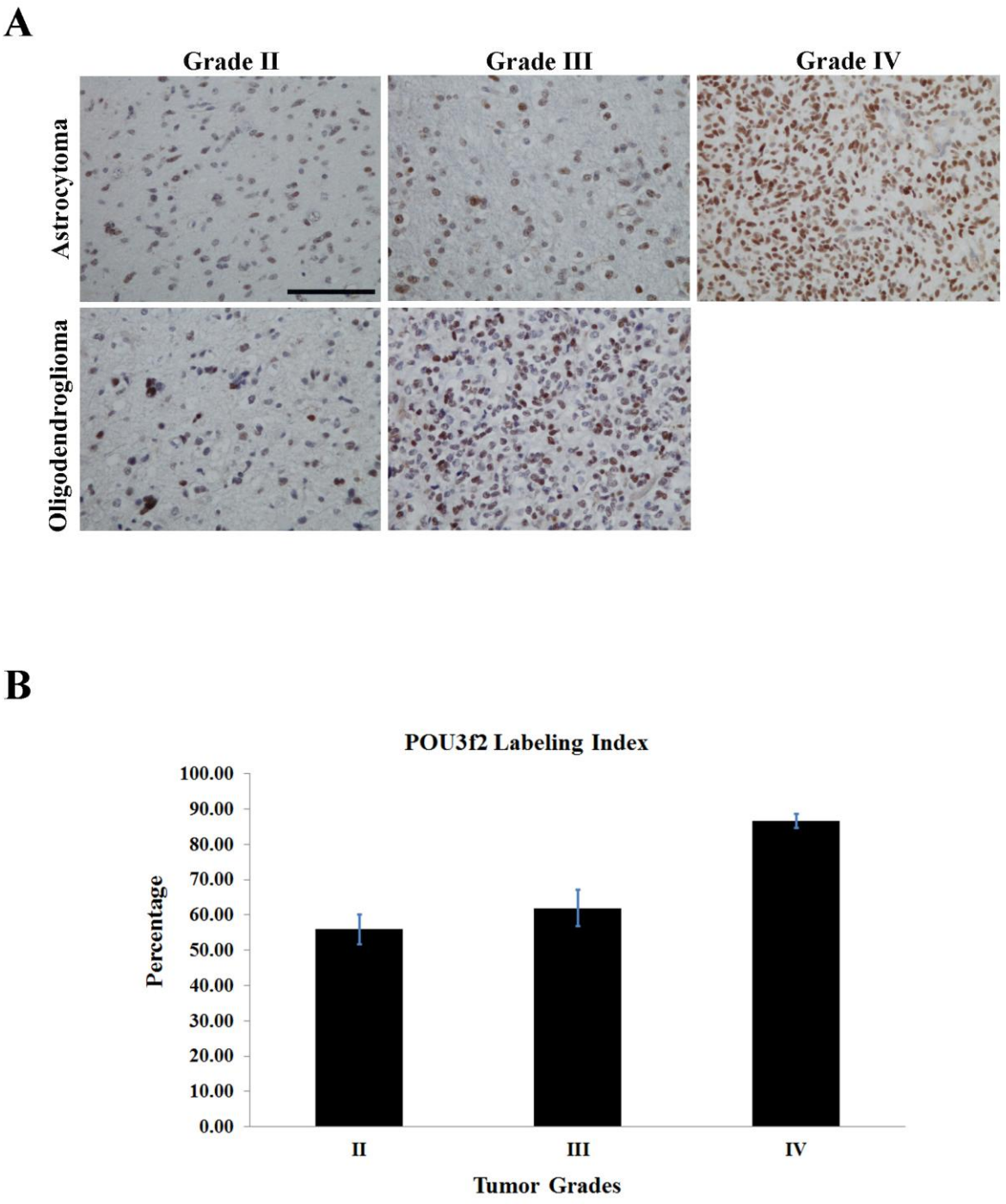

Figure 5.1.2.b POU3f2 staining and average of labeling index. A. IHC staining of POU3f2 in grade II-IV astrocytoma and grade II and III oligodendroglioma**.** All the images are shown with 40x magnification and scale bar = 50µm. **B.** Average of labeling index for the three grades of glioma (51 patients). Error bars :SEM

5.2 Immunobloting result for expression pattern of POU3f2 in gliomas patients

In order to validate POU3f2 expression on protein levels through an alternative method I performed western blotting for POU3f2 expression in 37 human glioma biopsies (12 grade II gliomas, 12 grade III gliomas and 13 grade IV gliomas) (Fig. 5.2 A). The POU3f2 protein was expressed in all of the samples and displayed a band at 55 kDa in all grades. The average relative signal intensity for POU3f2 compared to GAPDH was calculated for each

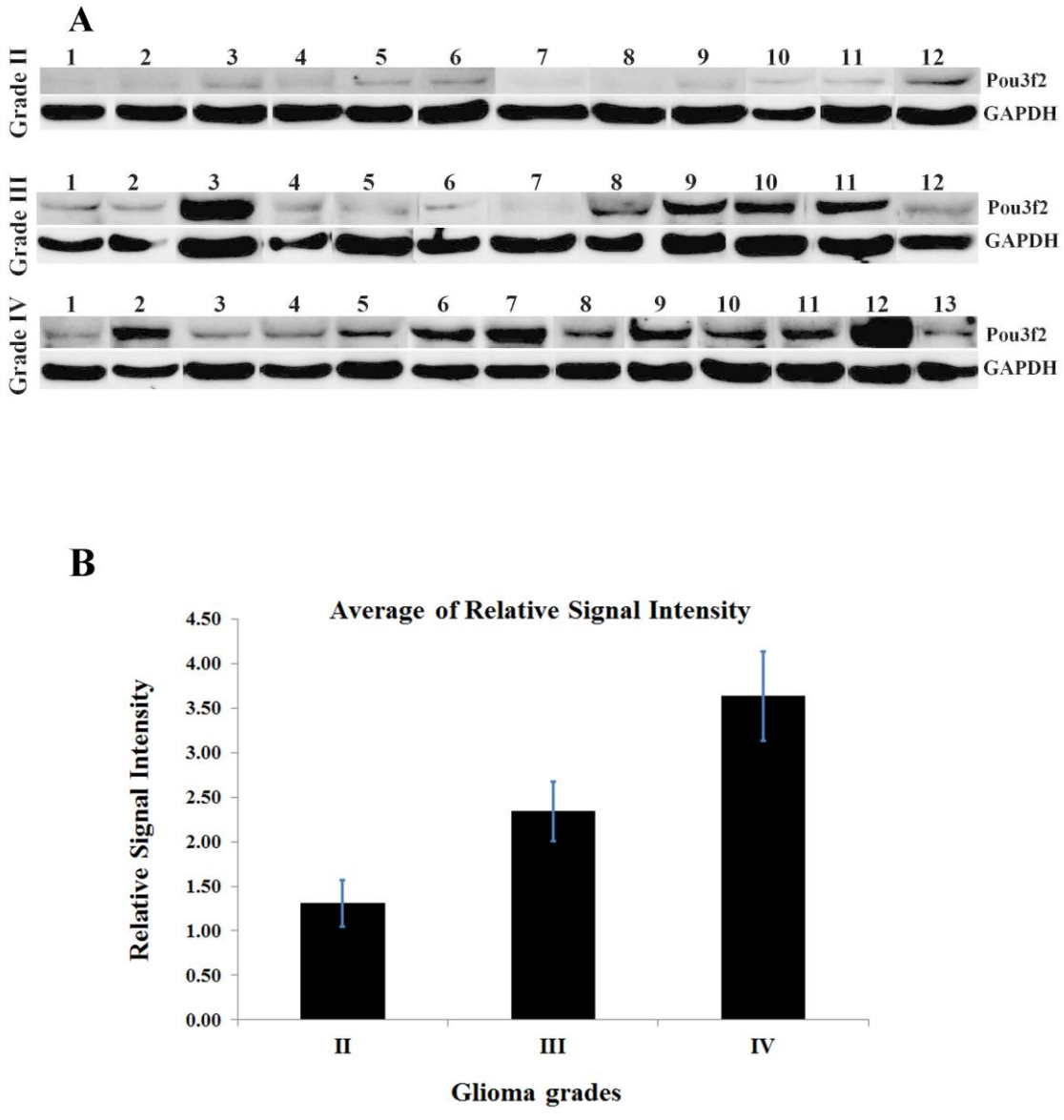

Figure 5.2 Immunoblotting analysis of POU3f2 in a panel of 37 gliomas patients. A. The POU3f2 bands were detected in all patients at 55 kDa, and GAPDH bands were detected at approximately 40 kDa. **B.** Average of relative signal intensity of western blotting for grades II, III and IV of glioma. Error bars: SEM

grade separately (Fig. 5.2 A). The signal intensities were 1.31 (+/- 0.26 SE) for grade II, 2.34 (+/-0.33 SE) for grade III and 3.63 (+/-0.50 SE) for grade IV gliomas. Thus, POU3f2 expression as measured by western blotting, increased with tumor grade, displaying significant differences between each tumor grade (Fig. 5.2 B). Protein expression levels on Western blot was significantly different between the groups (P-value = 0.0009, Kruskal-Wallis). Upon multiple testing, we found that the POU3f2 was significantly higher in grade IV than grade II gliomas ($0.001 > P > 0.0001$).

5.3 Expression of POU3f2 investigated by qRT-PCR

5.3.1 RNA quality

RNA was extracted from 38 patient samples to analyze POU3f2 RNA expression and the RNA quality (Section 4.7.4) was assessed by gel electrophoresis. The following criteria had to be fulfilled: 1) The bands representing, ribosomal subunits (18S and 28S) should be clear and 2) The intensity of 28S band should be approximately double that of 18S[113] (Fig 5.3.1). Of these, 10 samples showed no detectable band or had poorly defined bands suggesting RNA degradation; for these samples, new tissue was collected again and RNA extraction was repeated until a good quality of RNA was obtained.

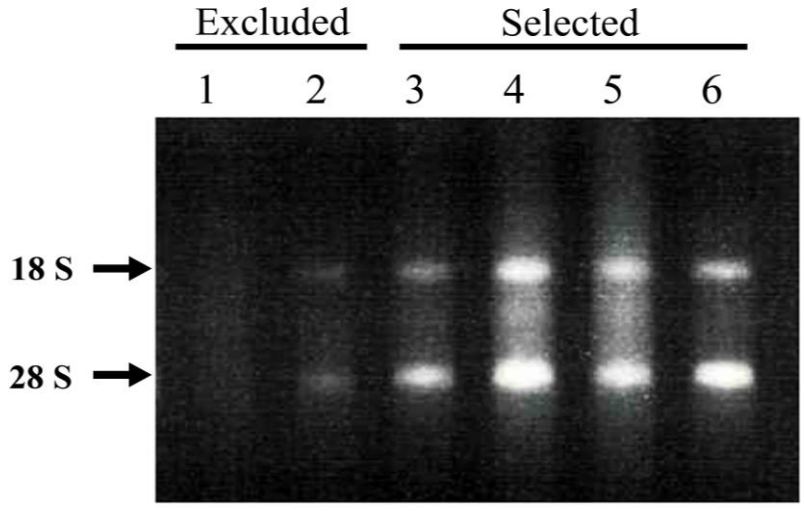

Figure 5.3.1 Gel electrophoresis of RNA samples extracted from human glioma samples. The samples 3, 4, 5, 6 were regarded to have RNA of good quality, whereas the samples in lane 1 and 2 were not.

5.3.2 Detection of POU3f2 and quantification of POU3f2 expression levels by qRT-PCR

The rate of POU3f2 expression was determined in different grades of gliomas (grade II, III, IV) by qRT-PCR, and the fold changes were calculated (all the samples were compared with one of the grade II patients, patient number 6). Moreover, POU3f2 RNA expression levels were correlated with tumor grades and subsequently compared with expression levels of POU3f2 as determined by immunoblotting and IHC.

Melt curves illustrated the same point in all the samples suggesting amplification of a specific target during the qRT-PCR experiment. Some representative quantifications and melt curves are illustrated in figure 5.3.2.a B.

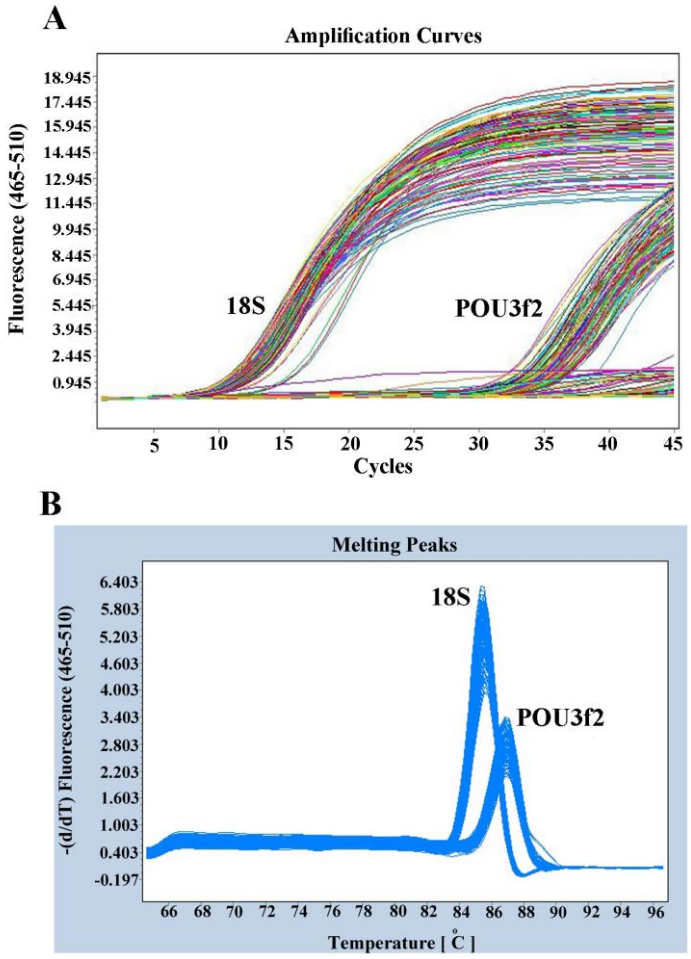

Figure 5.3.2.a Representative quantifications and melt curves of qRT-PCR: **A.** 18S and POU3f2 Ct values in glioma patients: The X-axis shows the number of cycles, and relative fluorescence units (RFU) are shown on the y-axis. **B:** Melt curves for 18S and POU3f2 fragment: Melt curves show a single peak for each product indicating amplification of a specific product during qRT-PCR. The X-axis displays temperature (ºC) and the y-axis displays –d(RFU)/dT (d=derived).

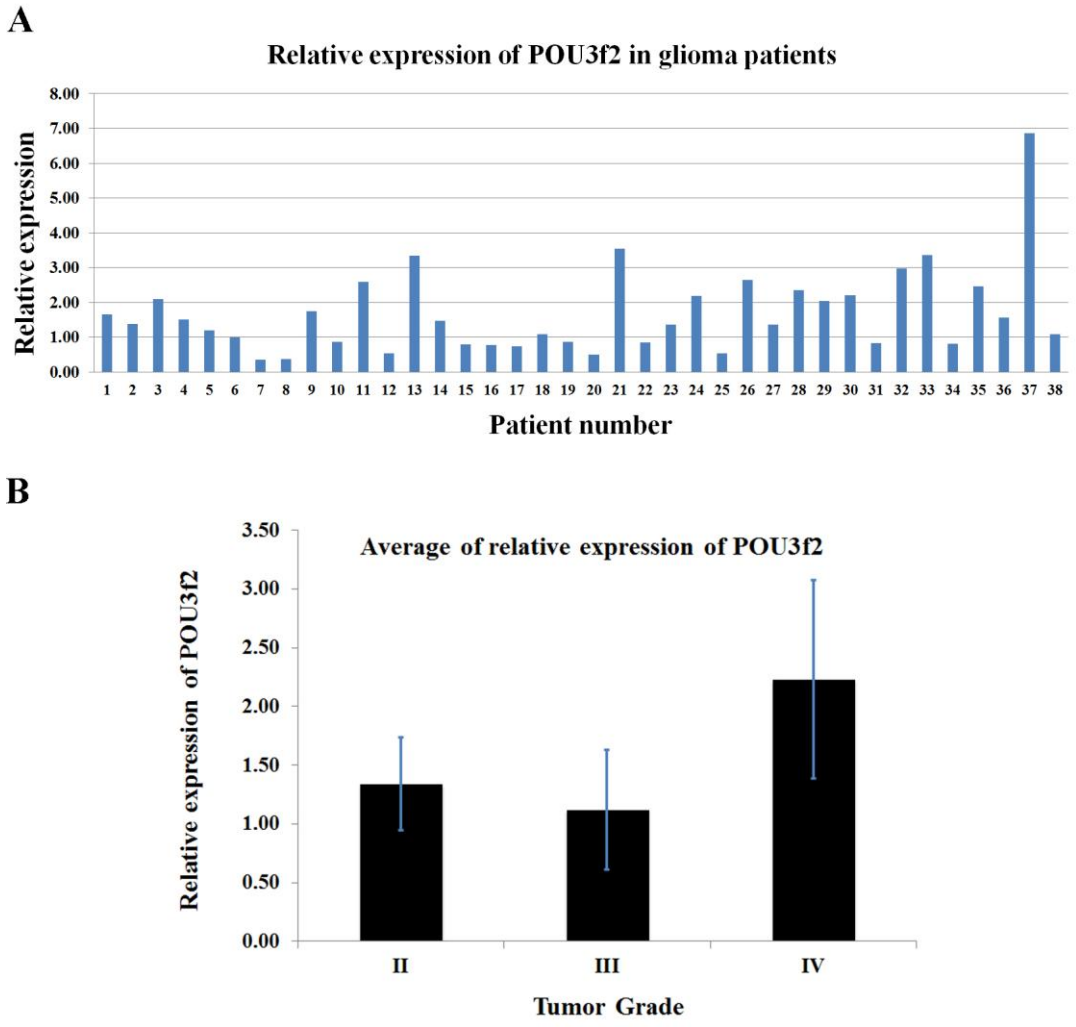

Figure 5.3.2.b Relative expression of POU3f2 in human glioma patients. A. Relative expression of POU3f2 in each patient: numbers 1-12 are grade II, numbers 13-24 are grade III and numbers 25-38 are grade IV. **B.** The average relative expression of POU3f2 in gliomas patients: The average relative expression of POU3f2 with standard error of the mean is displayed. Expression of POU3f2 was normalized by the housekeeping gene 18S.

Notably, the qRT-PCR experiments confirmed the IHC and western blotting experiments, showing that POU3f2 was widely expressed in gliomas (Fig 5.3.2.a A, 5.3.2.b A). Moreover, we again found that POU3f2 expression correlated with tumor grading (Fig 5.3.2.b B). The POU3f2 expression on qPCR also differed significantly between the groups (P-value = 0.02, Kruskal-Wallis)). Notably Grade IV tumors displayed a significantly higher POU3f2 expression (average normalized expression 2.23 (+/- 0.84 SE)) than grade III gliomas (Average normalized expression 1.12 (+/- 0.51 SE), P = 0.03). Although expression of POU3f2 between grade II (average normalized expression 1.34 (+/-0.39 SE)) was lower than in grade III and IV gliomas these differences were not significant.

5.4 Functional role of the POU3f2

The almost uniform expression of POU3f2 in gliomas that increased with tumor grade, suggested that POU3f2 may have a role in brain tumor progression. Thus, we performed a series of experiments to investigate how POU3f2 impacted on various aspects of glioma cell behavior.

5.4.1 Establishment of U251 glioma cell lines with constitutive overexpression or silencing of POU3f2

First, we used lentiviral vectors with plasmids encoding POU3f2, blank vector, POU3f2 siRNA and scrambled siRNA to obtain U251 glioma cell lines with overexpression or downregulation of POU3f2 as well as U251 expressing blank vector and scrambled siRNA. U251 is a commonly used glioma cell line, displaying low constitutive POU3f2 expression (Fig 5.4.1.e). U251 wild type cells were infected by different plasmids according to the protocol explained in section 4.8. All the plasmids also contained GFP (green fluorescent protein) and the puromycin phosphotransferase gene mediating puromycin resistance. The cells that contained these two genes had resistance against puromycin (via puromycin

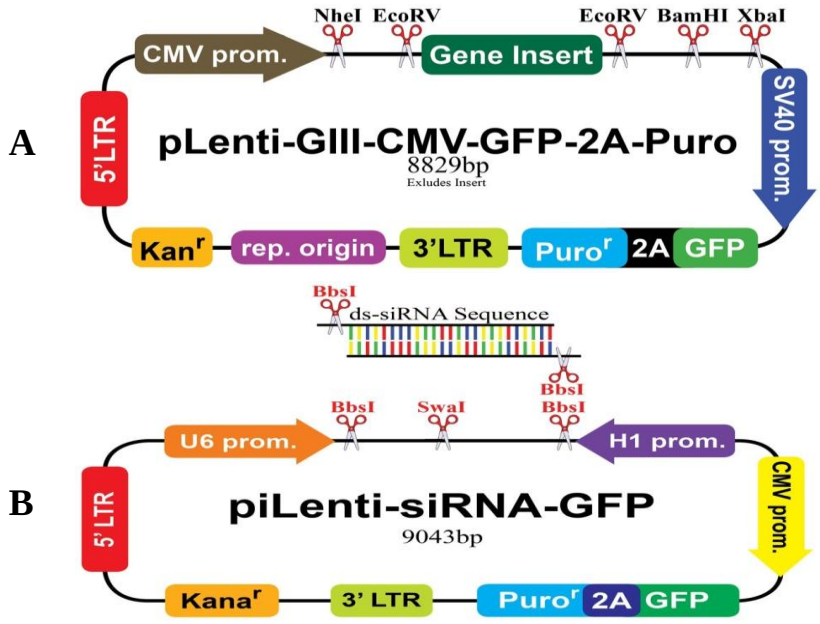

Figure 5.4.1.a Map of plasmids in POU3f2 overexpressor and POU3f2 siRNA construct. A: Plenti-POU3f2-GIII-CMV-GFP-2A-Puro is a POU3f2 overexpressor plasmid. Moreover, pLenti-CMV-GFP-2A-Puro-Blank was used as a control for the POU3f2 overexpressor. The structure of the blank-plasmid was same as the overexpressor plasmid, but it did not contain gene sequence. **B.** piLenti-POU3f2-siRNA-GFP is a siRNA plasmid. All the plasmid contained a GFP-2A-puro sequence. Subsequently, they were resistant to the puromycin and were able to express Green fluoresces protein as a marker.

phosphotransferase) and were fluoresce green (via GFP). Therefore, transfected cell lines were obtained by adding puromycin. The GFP makes it possible to distinguish between cells with/without vectors because surviving cells (after antibiotic treatment) are also positive for GFP.

The gene arrangements in plasmids are shown in figure 5.4.1.a, these plasmids were used for establishing different cell lines.

Interest plasmids were transformed in *E.coli* and after amplification, the plasmids were extracted from bacteria colonies. Digested plasmid DNA was run on 1% agarose gel (section 4.8.3) and result of the gel electrophoresis showed that the plasmids contained a DNA fragment of interest confirming that cloning was successful in all samples (FIG 5.4.1.b)

Next, these plasmids were used for making a lentiviral virus (section 4.8.4) using the HEK 293T cell line. We then infected the U251 glioma cell line with lentiviral virus containing POU3f2, POU3f2 siRNA, blank vector and scrambled siRNA. The cell lines were treated with puromycin (1-10 µg/ml), and then the positive cells were sorted and collected by using FACS (fluorescence activated cell sorting). Stable transfectants of the U251 glioma cell line expressing the various transgenes are shown in figure 5.4.1.c.

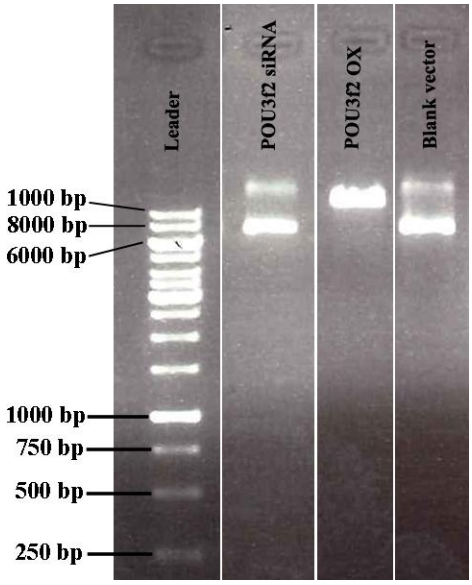

Figure 5.4.1.b. Control digestion of constructs. Plasmids from transformed bacteria were extracted and digested by a restriction enzyme (PstI (for pLenti-POU3f2-GFP and pLenti-GFP), SmaI (for pLenti-POU3f2 siRNA-GFP)). The digested DNA was run on a 1% agarose gel. The correct bands were observed on the gel for all the plasmids.

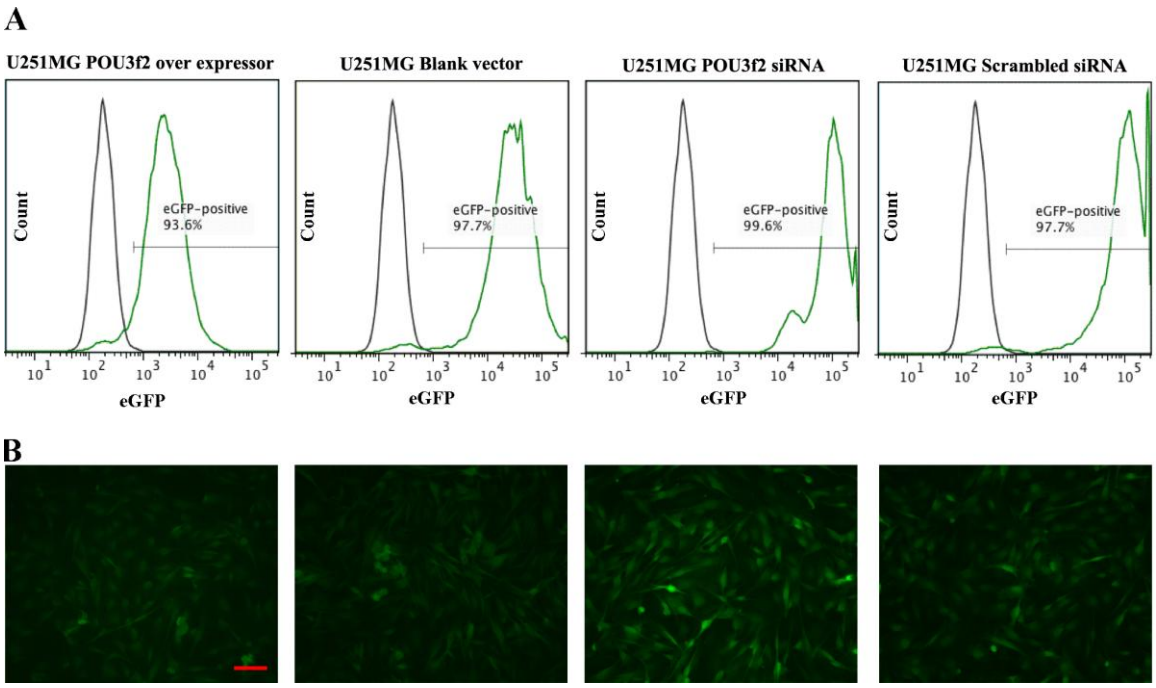

Figure 5.4.1.c: FACS analyzed infected cells. A. After transfection, Flow Cytometry was used to collect the GFP-positive cells. The percentage of GFP-positive cells for each cell line is illustrated in the graphs. The wild type cell line was used as control. **B.** The pictures show U251 cell lines (U251 POU3f2 ox, Blank vector, U251 POU3f2 siRNA and U251 scrambled siRNA) after transduction. Magnification is 20x and Scale bar = 50µm.

To determine the percentage of overexpression and knock down, qRT-PCR and immunoblotting were performed; results demonstrated that POU3f2 was upregulated more than 6 fold in the POU3f2 overexpressing clone (U251 POU3f2 ox), whereas POU3f2 expression was reduced approximately 80% in the U251 POU3f2 knock down cell line (U251 POU3f2 siRNA) (5.4.1.d).

Knock down and over expression was also confirmed with ICC. The representative data is shown in figure 5.4.1.e. ICC results showed that all the cell lines (U251 wild type, U251 POU3f2 ox and U251 POU3f2 siRNA) are expressing POU3f2, but the amount of expression in the over expresser is higher than wild type while the knockdown cell line showed a lesser expression of POU3f2 in comparison with the wild type (Fig 5.4.1.e). The ICC results illustrated that POU3f2 is expressed in the nucleus (Fig 5.4.1.e). This data showed that the transfection of the cells was completely successful. These stable cell lines were used for following functional assay.

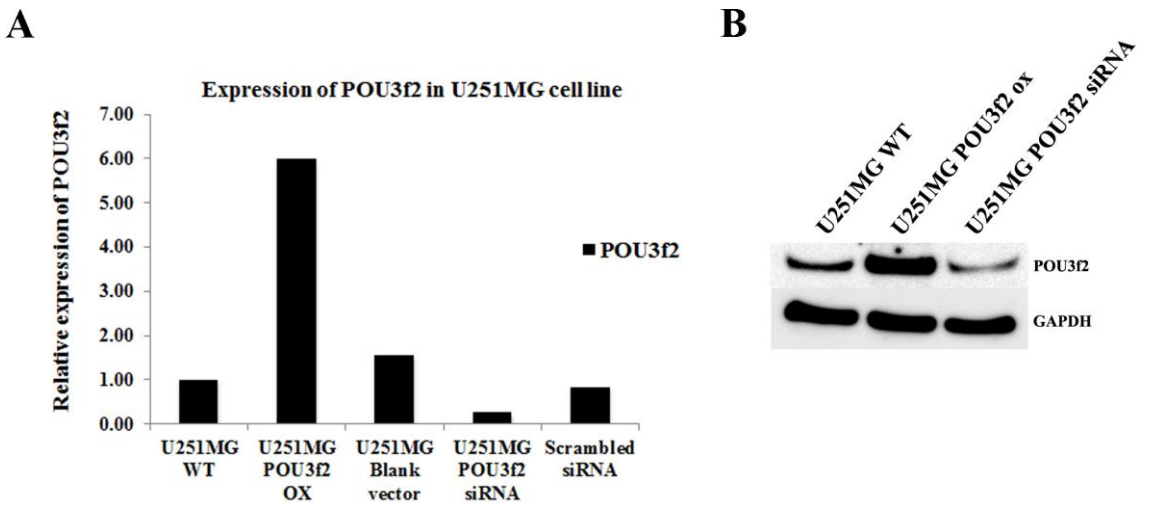

Figure 5.4.1.d POU3f2 expression was checked by qRT-PCR and western blot in U251 cell lines. A. POU3f2 expression level was investigated in U251 WT, U251 POU3f2 ox, U251 blank vector, U251 POU3f2 siRNA and U251 scrambled siRNA cell lines by qRT-PCR **B.** The rate of POU3f2 expression in U251 POU3f2 ox and U251 POU3f2 siRNA cell lines was checked by western blot.

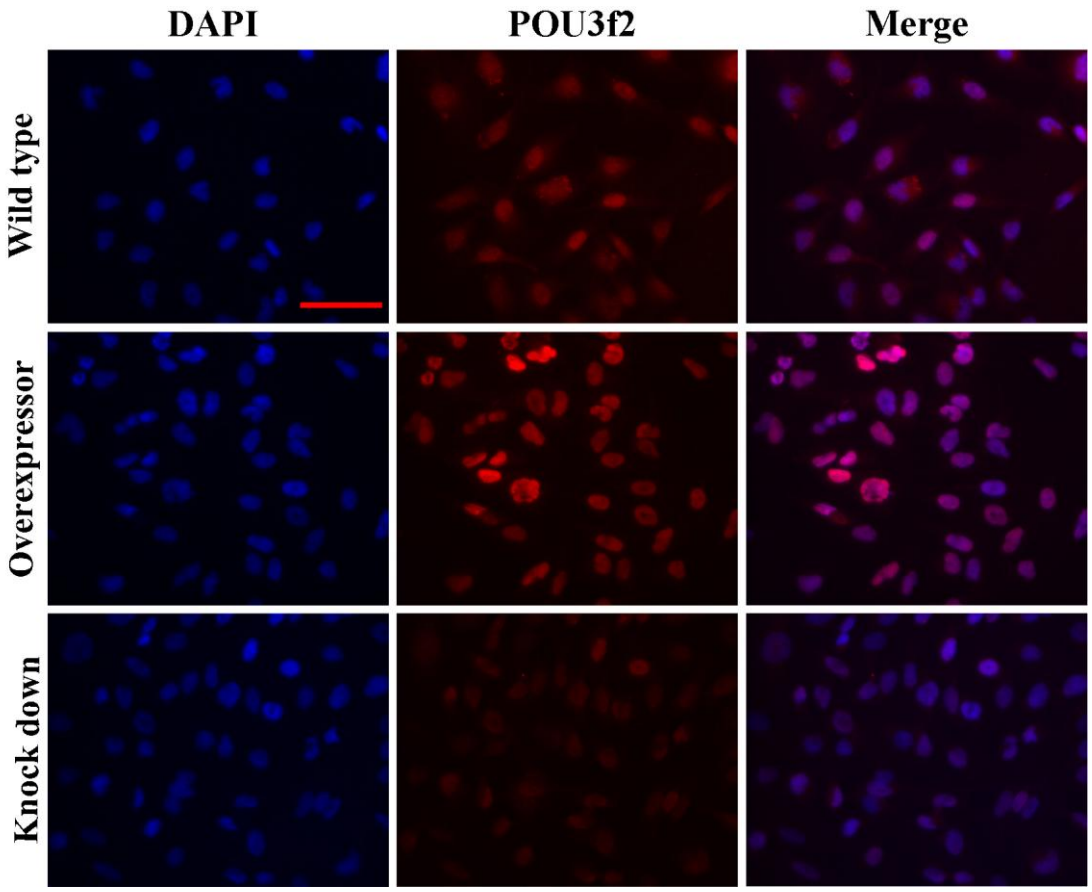

Figure 5.4.1.e Representative image of immunocytochemical staining using anti-POU3f2 in U251 cell lines. U251 Wild type, U251 POU3f2 ox and U251 POU3f2 siRNA cell lines are stained for POU3f2 by immunocytochemistry. POU3f2 staining (red) and nuclear counterstaining with DAPI (blue) as indicated. DAPI and POU3f2 staining is merged in the right panels, Scale bar = 50µm.

5.4.2 Proliferation assay

In order to investigate whether POU3f2 expression impacts on cell growth we monitored cell growth *in vitro* for the U251 WT, U251 POU3f2 ox, U251 POU3f2 siRNA, and U251 scrambled siRNA cell lines over 12 days. The proliferation assay was repeated two times for each cell line. Notably, the U251 POU3f2 ox cell line showed a higher growth rate with significantly higher cell numbers at day 9 and 12 (Fig 5.4.2). Between the other groups there were no significant differences (Fig 5.4.2).

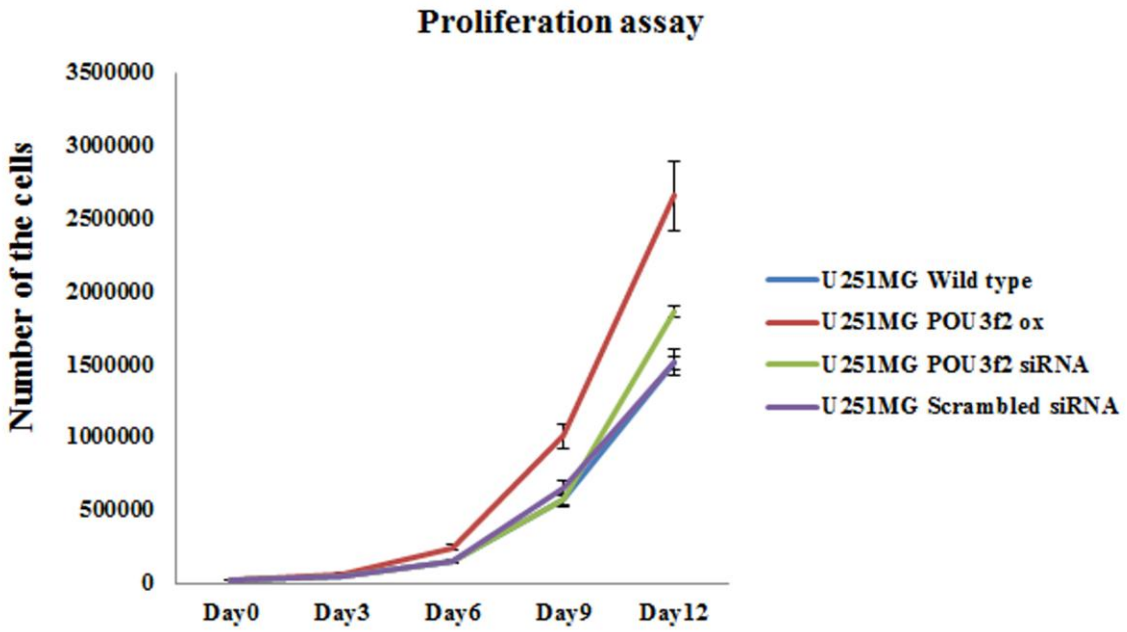

Figure 5.4.2 Representative data from a proliferation assay of U251 cell lines *in vitro* by manual counting. 15000 cells from different cell lines as indicated were seeded in each well and monitored until day 12. The U251 POU3f2 ox showed faster proliferation from day 9 in comparison to other cell lines. Error bars: SEM

5.4.3 Clonogenic assay

We then compared clonogenicity between the genetically modified U251 cell lines. Thus, 500 cells from each cell line were seeded in each well and cultured for 10 days. The cells were then stained, and the numbers of clones were counted. For the U251 POU3f2 ox (58 colony) cell line the clones were both more numerous and bigger in size than for the other cell lines which displayed few clones that were hardly visible macroscopically (Fig 5.4.3).

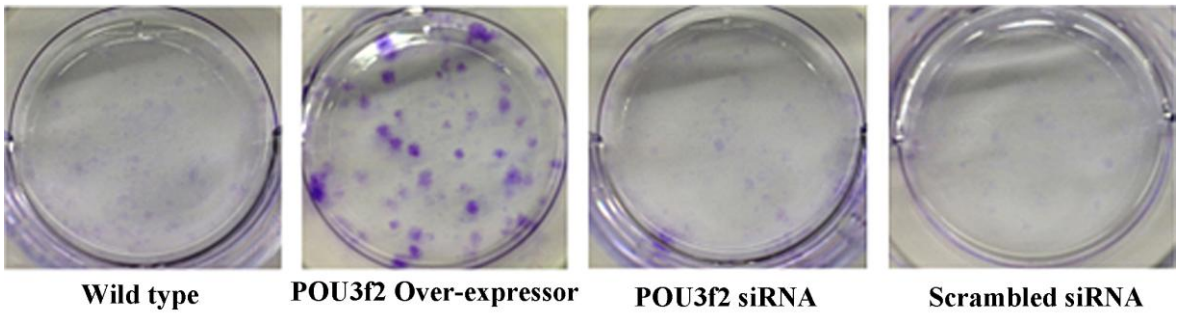

Figure 5.4.3 Results of clonogenic assay for U251 cell lines. 500 cells were seeded for each cell line and plates were incubated in a normoxia incubator for 10 days. The number of the colony in the U251 POU3f2 ox is significantly higher in compare to other cell lines.

5.5 Animal experiment

The U251 POU3f2 ox, U251 POU3f2 siRNA and U251 scrambled siRNA cell lines were also implanted into NOD-scid mice. Strikingly, all mice implanted with the U251 POU3f2 ox cell line developed large tumors and succumbed to their disease within 110 days, whereas all mice in the other groups at that time were healthy (5.5 B). A PET was performed with a radioactively labeled thymidine tracer (^{18}F)-FLT on one animal from each group at day 53 after implantation and showed a distinct uptake only in the mouse implanted with U251 POU3f2 ox, whereas uptake was barely detectable in mice from the other two groups (5.5 A). The study was terminated 150 days after implantation, and mice with U251 scrambled siRNA or POU3f2 siRNA were then asymptomatic.

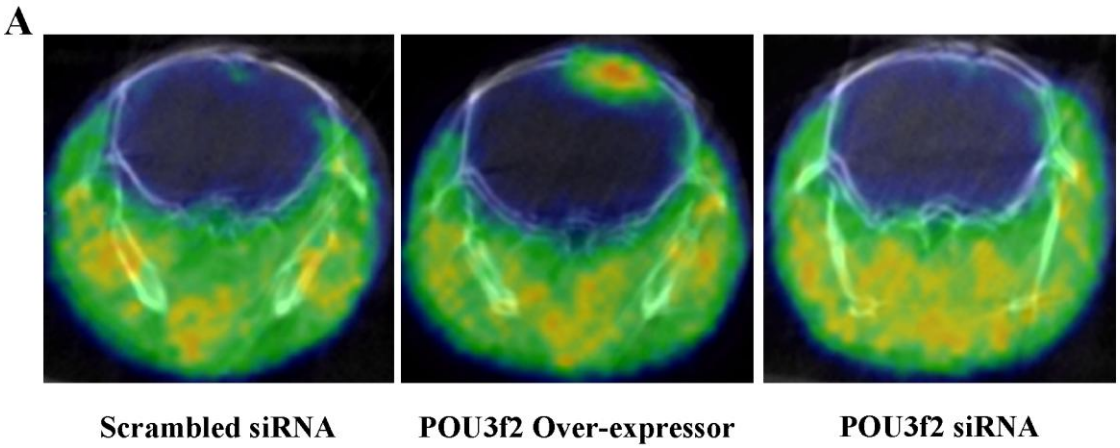

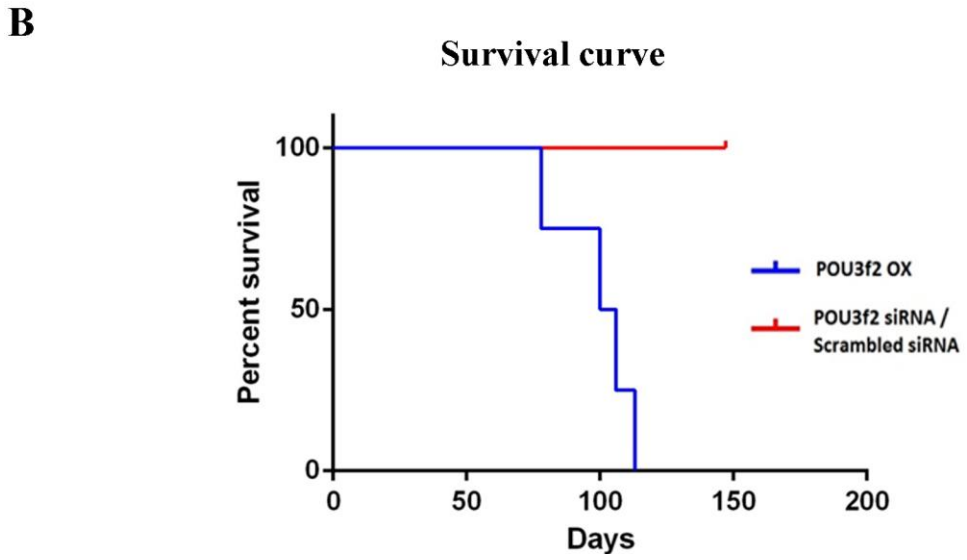

Figure 5.5 Result of PET scan. A. A PET scan performed on day 53 and showed a tumor for the overexpresser group **B.**Survival in NOD-scid mice following implantation with different U251 cell lines as indicated. The experiment was terminated at day 150. Mice implanted with either U251 POU3f2 siRNA or U251 scrambled siRNA were asymptomatic at this time point.

6. Discussion

Innumerable studies have reported deregulation and re-expression of embryonic transcription factors in different types of cancers, including gliomas. Notably, various fetal transcription factors such as SOX2, SOX6, SOX11, Oct4 and Nanog have been linked to glioma progression[65,114,115,116,117]. In some publications, co-expression of several of these factors has been reported in gliomas. For instance, Guo et al. reported that Oct4, SOX2 and Nanog were simultaneously expressed in glioma samples[65]. Furthermore, expression levels were higher in grade III and IV compared to grade II tumors[65]. Since POU3f2 is a CNS specific fetal transcription factor, we therefore wanted to investigate its expression in a series of human glioma and possibly its correlation with tumor grade.

6.1 Expression of POU3f2 in human glioma

In this study, we found that POU3f2 were expressed in the large majority of gliomas, increasingly with tumor grade. Expression of POU3f2 in an adult brain has been reported by Xi He et al., in 1989[88]; POU3f2 expression in adult rat brain is moderate while its expression in embryonic rat is quite high[88]. Furthermore, our IHC data was confirmed with both western blotting and qPCR which strengthens our data. Although Schreiber et al. reported the expression of N-oct-3 (POU3f2) in gliomas, his series contained only 7 malignant gliomas and expression was only investigated using western blotting[118]. Thus, POU3f2 expression has not previously been validated in a larger panel of human gliomas of different histological subclasses and across various grades using complementary methods. However, POU3f2 expression has been reported in melanomas [119,120,69], small cell lung cancer (SCLC)[97] and Retinoblastoma (RB)[102]. Notably, both retinoblastoma[121] and melanoma[122] arise from cells of neuroectodermal origin, similar to glioma cells[123]. Overexpression of POU3f2 is linked to progression of melanoma, and its expression is upregulated 10-fold in human melanoma cell lines compared to normal melanocytes[124]. Others have reported that POU3f2 is highly expressed in melanoblasts and melanomas while it is dramatically decreased in normal melanocytes[125]. In women diagnosed with renal cell carcinoma, those with POU3f2-positive tumors had a poorer survival outcome than women with POU3f2-negative tumors, while no correlation of POU3f2 status with overall survival was demonstrated in men[126]. Thus, it is possible that POU3f2 may also have a role during tumor progression in gliomas. The increasing expression of POU3f2 with tumor grade also suggests that POU3f2 contributes to

tumor aggressiveness. Thus, to investigate the clinical significance of POU3f2, expression levels should also be correlated with patient survival.

In this study, we used three different methods to investigate the expression of POU3f2. All methods showed that grade IV tumors expressed significantly higher levels of POU3f2 than at least one of the groups of lower grade tumors. However, whereas the IHC data showed significantly higher expression levels in grade IV tumors than both grade III and II tumors, western blotting showed higher expression in grade IV tumors only compared to grade II tumors and finally qPCR showed higher expression in grade IV tumors only compared to grade III tumors. Many factors may contribute to these findings. The most obvious reason is perhaps that these are different methods that measure expression by different criteria. Moreover, we did not have enough material to investigate the same samples with the three different methods. Thus, different samples were used for western blotting and qPCR and inter-individual variability between the patients may have contributed to our findings. It should be emphasized that the samples for the different analyses were picked randomly from the tumor bank before we knew result from any of the experiments. Thus, the selection of samples was not biased by knowledge of the POU3f2 expression from earlier analyses. Notably, the qPCR data differ from data obtained with the two other methods, as it showed higher expression (although not significant) in grade II than grade III tumors. However, the variability between the samples was much higher for the qPCR method, than for the other analyses. One possibility is that this variability reflects RNA degradation in some of the samples, since RNA is considerably more unstable than most proteins[127]. Thus, technical issues such as the quality of the samples may therefore also influence the results. In addition, transcription and translation is usually not linearly correlated, and posttranslational modifications may explain some of the observed discrepancy[128]. Notably, many of these different post-transcriptional processes involving protein synthesis are not well understood. Secondly, proteins have a varying half-life *in vivo* as some degrade more easily[127]. Thirdly, ribosomal density compare to number of RNA molecules has an effect on translation process[128]. .

Furthermore, different findings between the data from immunohistochemistry and western blotting may result from how these studies were designed. Usually, immunohistochemistry is considered a qualitative rather than a quantitative method. However, when staining is confined to the nucleus it is possible to estimate the labeling index for a sample based upon the fraction of immunopositive nuclei relative to all (immunopositive and –negative) nuceli.

This has proven useful for Ki67 staining of tumor sections as the Ki67 labelling index is a prognostic marker for certain cancer types. Since immunostaining was predominantly nuclear we therefore scored each section for its POU3f2 labelling index. However, this method does not take into account that some of the sections also displayed a cytoplasmic staining. In the western blot on the other hand, protein was extracted from the whole tissue and analysed. Therefore, in IHC rate of positive cells was calculated by checking POU3f2 expression in nucleus but in western blot cytoplasmic expression is also measured.

6.2 Functional assays of POU3f2

6.2.1 Proliferation assay

Overexpression of POU3f2 increased proliferation in U251, similar to what has previously been reported in melanoma cell lines[119]. Moreover, overexpression of POU3f2 enhanced proliferation in melanocytes[120]. Conversely, earlier studies have reported that downregulation of POU3f2 in melanoma cells decreased proliferation[120]. In melanoma cell lines, POU3f2 expression is reportedly regulated by different pathways such as Wnt/beta-catenin pathway, the RAS/RAF pathway, and the PI3K/AKT pathway[69]. Furthermore POU3f2 expression can be upregulated by amplification or modulation by miR-211 (in melanocytes)[69]. Upregulation and down-regulation of POU3f2 in SCLC cell lines and in melanoma increase and decrease proliferation activity respectively, albeit different mechanism is suggested for POU3f2 regulation in SCLC (Cobrinik et al., suggested that POU3f2 expression in SCLC is under control of the Rb gene) [91]. Currently, little is known about how POU3f2 expression is regulated in gliomas. It is worth noting that reexpression of wild type retinoblastoma (Rb) protein in Y79 retinoblastoma cell line strongly decreased expression of the POU3f2[102]. Thus, the Rb protein may have a role in regulating POU3f2 expression, which is disrupted in glioma and other cancers containing Rb mutations. It is important to point out that since we only have tested one glioma cell line so far, we do not know if POU3f2 consistently will increase proliferation in brain tumors.

6.2.2 Colony formation assay

Although cells divide during the observation period of a proliferation assay, they may still have a limited replicative potential. Thus, even among cancer cells there is only a fraction of

cells proliferating at a given time that have the ability to grow indefinitely. Clonogenic assays however, identifies cells giving rise to individual clones thereby reflecting potential for indefinite growth. Thus, we wanted to investigate whether POU3f2 also increased the clonogenicity of U251 cells in addition to proliferation. Therefore, we investigated the effect of overexpression and down-regulation of POU3f2 in a colony formation assay compared to various controls (U251 wild type and U251 scrambled siRNA). This experiment demonstrated that POU3f2 overexpression enhances clonogenicity, suggesting that the increased proliferation rates result from clonogenic cells and not only a number of transiently dividing cells. Furthermore, the other U251 cell lines formed small and poorly defined colonies. Because of this unconventional pattern of colony formation in the other cell lines and the fact that significant colony formation in the U251 POU3f2 overexpressor cell line was completely clear, plating efficiency was not calculated (Fig 5.4.3). Again, the limitation at this stage is the lack of confirmatory studies with additional glioma cell lines. However, similar experiments have recently been published but others who assessed the effects of forced overexpression of POU3f2 in differentiated glioblastoma cells (DGCs)[1] that have lost their sphere formation ability[129]. Notably, they reported that overexpression of POU3f2 in DGCs restored their ability to form spheroid in approximately 3% of the cells (compared to 0% for DCG expressing empty vector). Interestingly, co-expression of POU3f2 with SOX1/SOX2 enhanced spheroid formation even further, but was still not sufficient to mediate tumor formation *in vivo*[129].

6.2.3 Regional expression of POU3f2

IHC demonstrated that POU3f2 was predominantly localised to the nucleus, which is expected, given its role as a transcription factor. Yet POU3f2 we also observed cytoplasmic expression. Previously, cytoplasmic localization of POU3f2 has been reported in mouse spinal cord (in E13.5) while in the ventricular and subventricular zones, POU3f2 was observed in the nucleus[130,131]. In melanoma cell lines, expression of POU3f2 was reportedly limited to the nucleus[132] whereas cytoplasmic localization was observed in nevi. The authors suggested that this represented nucleocytoplasmic shuttling in melanocytic cells[68].

[1] Differentiated glioblastoma cells derived from human tumor and grown as adherent monolayers in serum, and they are not able to initiate tumor formation *in vivo*[129].

6.3 Effect of POU3f2 expression on glioma growth *in vivo*

Since POU3f2 is widely expressed in human gliomas, increasingly with tumor grade, we reasoned it might have a role in brain tumor progression. Moreover, our studies *in vitro* suggested that POU3f2 could increase proliferation and clonogenicity. We therefore wanted to investigate how POU3f2 affected growth *in vivo*, and found that overexpression of POU3f2 dramatically increased growth of the U251 cell line, compared to controls (U251 POU3f2 siRNA and U251 scrambled siRNA). Previously, Thomson et al., showed that human melanoma cell lines expressing antisense POU3f2 are not able to form tumors in immunodeficient mice[120,133], Similarly, we found that U251 POU3f2 siRNA did not form tumors. In the animals engrafted with U251 scrambled siRNA and U251 wild type tumors formed like previously reported by others[134]. However, the experiment was terminated towards the end of my laboratory period and these sections are still under ongoing analysis.

These results differ from those reported by Suva et al who did not find that overexpression of POU3f2 was sufficient to make DGCs tumorigenic in mice. In addition, when they co-expressed POU3f2 with SOX2 and SALL2 these cells could still not form tumor. However, with a combined overexpression of four transcription factors, POU3f2, SOX2, SALL2 and OLIG2 DGCs were able to form the tumor in mice[129]. These 4 transcription factors were sufficent to reprogram DGCs into induced stem-like tumor propagating cells (iTPCs) while it showed same properites as TPCs[2] (TPCs establised directly from human tumors)[129]. Since we found that overexpression of only POU3f2 was sufficient to significantly increased tumor formation it suggests that U251 may constitutively express additional factors necessary for tumor growth *in vivo*. Again, since we so far only have performed this study with one cell line, additional experiments are needed to conclude about the role of POU3f2 for tumor engraftment. Apart from, overexpressing POU3f2 in other cell lines, it is also important to investigate if cell lines that are tumorigenic when overexpressing POU3f2 also have a constitutive expression of other transcription factors in common.

Conclusion: In this study, we showed that POU3f2 expression was expressed in the large majority in a series of human glioma samples. Expression of POU3f2 in gliomas was grade dependent, as the expression of POU3f2 increased from lower to higher grade.

---

[2] Stem-like tumor propagating cells are derived from human tumor and grow in serum-free, spherogenic culture. These cells can form a tumor *in vivo*.

We demonstrated that, the over expression of POU3f2 in the U251 glioma cell line significantly increased proliferation and colony formation. On the other hand down regulation of POU3f2 decrease colony formation, but did not show a significant effect on proliferation.

In vivo experiment illustrated that overexpression of POU3f2 in U251 strongly promoted tumor growth, while knock-down abrogated the formation of macroscopically visible tumors upto 130 days after implantation. These data suggest that POU3f2 may play a pivotal role in glioma tumorigenesis, whereas the correlation with tumor grade may point to an involvement in glioma progression. We do not know whether it is a prognostic factor independent of tumor grade.

7. Future perspective

This study comprise both clinicopathological and functional data suggesting that the CNS specific fetal transcription POU3f2 may impact on multiple aspect of brain tumor growth and increase overall tumor aggressiveness. Due to the time constraints of this MSc project however, the functional data is limited to one glioma cell line. Further research should therefore expand these experiments to include additional glioma cell lines and preferably also primary tumor tissue. This way more extensive studies can be conducted both *in vitro* and *in vivo* and allow us to conclude with more certainty about the role of POU3f2 in brain tumor progression.

Furthermore, we know little about how POU3f2 expression is regulated in glioma and about which signaling pathways that are activated downstream. Findings reported by other suggest that POU3f2 may work in a coordinated manner with other transcriptiona factors.

8. References

1. Lahtz C, Pfeifer GP. Epigenetic changes of DNA repair genes in cancer. *J Mol Cell Biol*. 2011;3(1):51–8. doi:10.1093/jmcb/mjq053.

2. Croce CM. Oncogenes and cancer. *N Engl J Med*. 2008;358(5):502–11. doi:10.1056/NEJMra072367.

3. Milinkovic V, Bankovic J, Rakic M, et al. Identification of novel genetic alterations in samples of malignant glioma patients. *PLoS One*. 2013;8(12):e82108. doi:10.1371/journal.pone.0082108.

4. Macconaill LE, Garraway L a. Clinical implications of the cancer genome. *J Clin Oncol*. 2010;28(35):5219–28. doi:10.1200/JCO.2009.27.4944.

5. Kleihues, Paul WKCP., ed. *Pathology and Genetics Tumors of the Nervous System*. International Agency for Research on Cancer (IARC); 2000.

6. WHO: Cancer Fact Sheet Number 297. Edited by 2014,p.

7. Anand P, Kunnumakkara AB, Kunnumakara AB, et al. Cancer is a preventable disease that requires major lifestyle changes. *Pharm Res*. 2008;25(9):2097–116. doi:10.1007/s11095-008-9661-9.

8. Hanahan D, Weinberg R. The hallmarks of cancer. *Cell*. 2000;100(1):57–70. Available at: http://www.ncbi.nlm.nih.gov/pubmed/10647931. Accessed April 7, 2014.

9. Hanahan D, Weinberg R a. Hallmarks of cancer: the next generation. *Cell*. 2011;144(5):646–74. doi:10.1016/j.cell.2011.02.013.

10. Nishida N, Yano H, Nishida T, Kamura T, Kojiro M. Angiogenesis in cancer. *Vasc Health Risk Manag*. 2006;2(3):213–9. Available at: http://www.pubmedcentral.nih.gov/articlerender.fcgi?artid=1993983&tool=pmcentrez&rendertype=abstract. Accessed April 7, 2014.

11. Goodenberger ML, Jenkins RB. Genetics of adult glioma. *Cancer Genet*. 2012;205(12):613–21. doi:10.1016/j.cancergen.2012.10.009.

12. Louis DN, Holland EC, Cairncross JG. Glioma classification: a molecular reappraisal. *Am J Pathol*. 2001;159(3):779–86. doi:10.1016/S0002-9440(10)61750-6.

13. Huse JT, Holland EC. Targeting brain cancer: advances in the molecular pathology of malignant glioma and medulloblastoma. *Nat Rev Cancer*. 2010;10(5):319–31. doi:10.1038/nrc2818.

14. Maher E a, Furnari FB, Bachoo RM, et al. Malignant glioma: genetics and biology of a grave matter. *Genes Dev*. 2001;15(11):1311–33. doi:10.1101/gad.891601.

15. Louis DN, Ohgaki H, Wiestler OD, et al. The 2007 WHO classification of tumours of the central nervous system. *Acta Neuropathol*. 2007;114(2):97–109. doi:10.1007/s00401-007-0243-4.

16. Louis DN, Holland EC, Cairncross JG. Glioma classification: a molecular reappraisal. *Am J Pathol*. 2001;159(3):779–86. doi:10.1016/S0002-9440(10)61750-6.

17. Gonzales MF. Grading of gliomas. *J Clin Neurosci*. 1997;4(1):16–18. doi:10.1016/S0967-5868(97)90004-7.

18. Grier JT, Batchelor T. Low-grade gliomas in adults. *Oncologist*. 2006;11(6):681–93. doi:10.1634/theoncologist.11-6-681.

19. Huang H, Hara A, Homma T, Yonekawa Y, Ohgaki H. Altered expression of immune defense genes in pilocytic astrocytomas. *J Neuropathol Exp Neurol*. 2005;64(10):891–901. Available at: http://www.ncbi.nlm.nih.gov/pubmed/16215461. Accessed December 2, 2013.

20. Pallud J, Fontaine D, Duffau H, et al. Natural history of incidental World Health Organization grade II gliomas. *Ann Neurol*. 2010;68(5):727–33. doi:10.1002/ana.22106.

21. Møller HG, Rasmussen AP, Andersen HH, Johnsen KB, Henriksen M, Duroux M. A systematic review of microRNA in glioblastoma multiforme: micro-modulators in the mesenchymal mode of migration and invasion. *Mol Neurobiol*. 2013;47(1):131–44. doi:10.1007/s12035-012-8349-7.

22. Meyer M a. Malignant gliomas in adults. *N Engl J Med*. 2008;359(17):1850; author reply 1850. doi:10.1056/NEJMc086380.

23. Nikiforova MN, Hamilton RL. Molecular diagnostics of gliomas. *Arch Pathol Lab Med*. 2011;135(5):558–68. doi:10.1043/2010-0649-RAIR.1.

24. Ostrom QT, Gittleman H, Farah P, et al. CBTRUS statistical report: Primary brain and central nervous system tumors diagnosed in the United States in 2006-2010. *Neuro Oncol*. 2013;15 Suppl 2:ii1–56. doi:10.1093/neuonc/not151.

25. International Agency for Research on Cancer. GLOBOCAN 2012, Estimated Cancer Incidence, Mortality and Prevalence Worldwide in 2012: IARC: International Agency for Research on Cancer; Year. Available at: http://globocan.iarc.fr/.

26. Bondy ML, Scheurer ME, Malmer B, et al. Brain tumor epidemiology: consensus from the Brain Tumor Epidemiology Consortium. *Cancer*. 2008;113(7 Suppl):1953–68. doi:10.1002/cncr.23741.

27. Schwartzbaum J, Fisher J. Epidemiology and molecular pathology of glioma. *Nat Clin Pract …*. 2006;2(9):494–503; quiz 1 p following 516. doi:10.1038/ncpneuro0289.

28. Ohgaki H, Kleihues P. Genetic pathways to primary and secondary glioblastoma. *Am J Pathol*. 2007;170(5):1445–53. doi:10.2353/ajpath.2007.070011.

29. Liu X-Y, Gerges N, Korshunov A, et al. Frequent ATRX mutations and loss of expression in adult diffuse astrocytic tumors carrying IDH1/IDH2 and TP53 mutations. *Acta Neuropathol*. 2012;124(5):615–25. doi:10.1007/s00401-012-1031-3.

30. Ohgaki H. Genetic pathways to glioblastomas. *Neuropathology*. 2005;25(1):1–7. Available at: http://www.ncbi.nlm.nih.gov/pubmed/15466178. Accessed December 20, 2013.

31. Ohgaki H, Kleihues P. Population-based studies on incidence, survival rates, and genetic alterations in astrocytic and oligodendroglial gliomas. *J Neuropathol Exp Neurol*. 2005;64(6):479–89. Available at: http://www.ncbi.nlm.nih.gov/pubmed/15977639. Accessed December 4, 2013.

32. Sanson M, Thillet J, Hoang-Xuan K. Molecular changes in gliomas. *Curr Opin Oncol*. 2004;16(6):607–13. Available at: http://www.ncbi.nlm.nih.gov/pubmed/21029244.

33. Balss J, Meyer J, Mueller W, Korshunov A, Hartmann C, von Deimling A. Analysis of the IDH1 codon 132 mutation in brain tumors. *Acta Neuropathol*. 2008;116(6):597–602. doi:10.1007/s00401-008-0455-2.

34. Bralten LBC, French PJ. Genetic alterations in glioma. *Cancers (Basel)*. 2011;3(1):1129–40. doi:10.3390/cancers3011129.

35. Nupponen NN, Joensuu H. Molecular pathology of gliomas. *Curr Diagnostic Pathol*. 2006;12(5):394–402. doi:10.1016/j.cdip.2006.06.007.

36. Wemmert S, Romeike BFM, Ketter R, Steudel W-I, Zang KD, Urbschat S. Intratumoral genetic heterogeneity in pilocytic astrocytomas revealed by CGH-analysis of microdissected tumor cells and FISH on tumor tissue sections. *Int J Oncol*. 2006;28(2):353–60. Available at: http://www.ncbi.nlm.nih.gov/pubmed/16391789.

37. Van den Bent MJ, Reni M, Gatta G, Vecht C. Oligodendroglioma. *Crit Rev Oncol Hematol*. 2008;66(3):262–72. doi:10.1016/j.critrevonc.2007.11.007.

38. Zuber P, Hamou MF, de Tribolet N. Identification of proliferating cells in human gliomas using the monoclonal antibody Ki-67. *Neurosurgery*. 1988;22(2):364–8. Available at: http://www.ncbi.nlm.nih.gov/pubmed/2832782. Accessed April 16, 2014.

39. Jouanneau E. Angiogenesis and gliomas: current issues and development of surrogate markers. *Neurosurgery*. 2008;62(1):31–50; discussion 50–2. doi:10.1227/01.NEU.0000311060.65002.4E.

40. Gupta M, Djalilvand A, Brat DJ. Clarifying the Diffuse Gliomas: An Update on the Morphologic Features and Markers That Discriminate Oligodendroglioma From Astrocytoma. *Am J Clin Pathol*. 2005;124(5):755–768. doi:10.1309/6JNX4PA60TQ5U5VG.

41. Beauchesne P. Extra-neural metastases of malignant gliomas: myth or reality? *Cancers (Basel)*. 2011;3(1):461–77. doi:10.3390/cancers3010461.

42. Armstrong TS. Head's up on the treatment of malignant glioma patients. *Oncol Nurs Forum*. 2009;36(5):E232–40. doi:10.1188/09.ONF.E232-E240.

43. Ferguson SD. Malignant gliomas: diagnosis and treatment. *Dis Mon*. 2011;57(10):558–69. doi:10.1016/j.disamonth.2011.08.020.

44. Meyer M a. Malignant gliomas in adults. *N Engl J Med*. 2008;359(17):1850; author reply 1850. doi:10.1056/NEJMc086380.

45. Philip-Ephraim EE, Eyong KI, Williams UE, Ephraim RP. The role of radiotherapy and chemotherapy in the treatment of primary adult high grade gliomas: assessment of patients for these treatment approaches and the common immediate side effects. *ISRN Oncol*. 2012;2012:902178. doi:10.5402/2012/902178.

46. Whittle IR. The dilemma of low grade glioma. *J Neurol Neurosurg Psychiatry*. 2004;75(suppl_2):ii31–ii36. doi:10.1136/jnnp.2004.040501.

47. Claes A, Idema AJ, Wesseling P. Diffuse glioma growth: a guerilla war. *Acta Neuropathol*. 2007;114(5):443–58. doi:10.1007/s00401-007-0293-7.

48. Duncan JS, de Tisi J. MRI in the diagnosis and management of epileptomas. *Epilepsia*. 2013;54 Suppl 9:40–3. doi:10.1111/epi.12442.

49. Grier JT, Batchelor T. Low-grade gliomas in adults. *Oncologist*. 2006;11(6):681–93. doi:10.1634/theoncologist.11-6-681.

50. Deimling A Von. *Gliomas*. (Deimling A, ed.). Berlin, Heidelberg: Springer Berlin Heidelberg; 2009. doi:10.1007/978-3-540-31206-2.

51. Nitta T, Sato K. Prognostic implications of the extent of surgical resection in patients with intracranial malignant gliomas. *Cancer*. 1995;75(11):2727–31. Available at: http://www.ncbi.nlm.nih.gov/pubmed/7743477. Accessed April 14, 2014.

52. Ammirati M, Vick N, Liao YL, Ciric I, Mikhael M. Effect of the extent of surgical resection on survival and quality of life in patients with supratentorial glioblastomas and anaplastic astrocytomas. *Neurosurgery*. 1987;21(2):201–6. Available at: http://www.ncbi.nlm.nih.gov/pubmed/2821446. Accessed April 14, 2014.

53. Sadighi Z, Slopis J. Pilocytic astrocytoma: a disease with evolving molecular heterogeneity. *J Child Neurol*. 2013;28(5):625–32. doi:10.1177/0883073813476141.

54. Lonardi S, Tosoni A, Brandes A a. Adjuvant chemotherapy in the treatment of high grade gliomas. *Cancer Treat Rev*. 2005;31(2):79–89. doi:10.1016/j.ctrv.2004.12.005.

55. Van den Bent MJ. Adjuvant treatment of high grade gliomas. *Ann Oncol*. 2006;17 Suppl 1(Supplement 10):x186–90. doi:10.1093/annonc/mdl258.

56. Paleologos N a, Merrell RT. Anaplastic glioma. *Curr Treat Options Neurol*. 2012;14(4):381–90. doi:10.1007/s11940-012-0177-6.

57. Brada M. Phase II study of primary temozolomide chemotherapy in patients with WHO grade II gliomas. *Ann Oncol*. 2003;14(12):1715–1721. doi:10.1093/annonc/mdg371.

58. Friedman H, Kerby T, Calvert H. Temozolomide and treatment of malignant glioma. *Clin Cancer Res*. 2000;6(7):2585–97. Available at: http://www.ncbi.nlm.nih.gov/pubmed/10914698. Accessed May 31, 2014.

59. Bromberg JEC, van den Bent MJ. Oligodendrogliomas: molecular biology and treatment. *Oncologist*. 2009;14(2):155–63. doi:10.1634/theoncologist.2008-0248.

60. Tham CK, See SJ, Tan SH, et al. Combined temozolomide and radiation as an initial treatment for anaplastic glioma. *Asia Pac J Clin Oncol*. 2013;9(3):220–5. doi:10.1111/ajco.12038.

61. Meyer M a. Malignant gliomas in adults. *N Engl J Med*. 2008;359(17):1850; author reply 1850. doi:10.1056/NEJMc086380.

62. Bai R-Y, Staedtke V, Riggins GJ. Molecular targeting of glioblastoma: Drug discovery and therapies. *Trends Mol Med*. 2011;17(6):301–12. doi:10.1016/j.molmed.2011.01.011.

63. Ma Y, Zhang P, Wang F, Yang J, Yang Z, Qin H. The relationship between early embryo development and tumourigenesis. *J Cell Mol Med*. 2010;14(12):2697–701. doi:10.1111/j.1582-4934.2010.01191.x.

64. Monk M, Holding C. Human embryonic genes re-expressed in cancer cells. *Oncogene*. 2001;20(56):8085–91. doi:10.1038/sj.onc.1205088.

65. Guo Y, Liu S, Wang P, et al. Expression profile of embryonic stem cell-associated genes Oct4, Sox2 and Nanog in human gliomas. *Histopathology*. 2011;59(4):763–75. doi:10.1111/j.1365-2559.2011.03993.x.

66. Holmberg J, He X, Peredo I, et al. Activation of neural and pluripotent stem cell signatures correlates with increased malignancy in human glioma. *PLoS One*. 2011;6(3):e18454. doi:10.1371/journal.pone.0018454.

67. Kondo T. Brain cancer stem-like cells. *Eur J Cancer*. 2006;42(9):1237–42. doi:10.1016/j.ejca.2006.01.038.

68. Cook AL, Sturm R a. POU domain transcription factors: BRN2 as a regulator of melanocytic growth and tumourigenesis. *Pigment Cell Melanoma Res*. 2008;21(6):611–26. doi:10.1111/j.1755-148X.2008.00510.x.

69. Besch R, Berking C. POU transcription factors in melanocytes and melanoma. *Eur J Cell Biol*. 2013:1–6. doi:10.1016/j.ejcb.2013.10.001.

70. LEONG S. *From Melanocytes to Melanoma*. (Hearing VJ, Leong SPL, eds.). Totowa, NJ: Humana Press; 2006:149–167. doi:10.1007/978-1-59259-994-3.

71. Herr W, Cleary M a. The POU domain: versatility in transcriptional regulation by a flexible two-in-one DNA-binding domain. *Genes Dev*. 1995;9(14):1679–1693. doi:10.1101/gad.9.14.1679.

72. Verrijzer CP, Van der Vliet PC. POU domain transcription factors. *Biochim Biophys Acta*. 1993;1173(1):1–21. Available at: http://www.ncbi.nlm.nih.gov/pubmed/8485147. Accessed January 12, 2014.

73. Wegner M, Drolet DW, Rosenfeld MG. POU-domain proteins: structure and function of developmental regulators. *Curr Opin Cell Biol*. 1993;5(3):488–98. Available at: http://www.ncbi.nlm.nih.gov/pubmed/8352967. Accessed January 7, 2014.

74. Ryan a K, Rosenfeld MG. POU domain family values: flexibility, partnerships, and developmental codes. *Genes Dev*. 1997;11(10):1207–1225. doi:10.1101/gad.11.10.1207.

75. Wright PE. POU domains and homeodomains. *Curr Opin Struct Biol*. 1994;4(1):22–27. doi:10.1016/S0959-440X(94)90055-8.

76. Veenstra GJ, van der Vliet PC, Destrée OH. POU domain transcription factors in embryonic development. *Mol Biol Rep*. 1997;24(3):139–55. Available at: http://www.ncbi.nlm.nih.gov/pubmed/9291088. Accessed March 19, 2014.

77. Shi G, Jin Y. Role of Oct4 in maintaining and regaining stem cell pluripotency. *Stem Cell Res Ther*. 2010;1(5):39. doi:10.1186/scrt39.

78. Rosner M, Vigano M, Ozato K. A POU-domain transcription factor in early stem cells and germ cells of the mammalian embryo. *Nature*. 1990;345(6277):686–92. doi:10.1038/345686a0.

79. Andersen B, Rosenfeld MG. POU domain factors in the neuroendocrine system: lessons from developmental biology provide insights into human disease. *Endocr Rev*. 2001;22(1):2–35. doi:10.1210/edrv.22.1.0421.

80. Pesce M, Wang X, Wolgemuth DJ, Schöler H. Differential expression of the Oct-4 transcription factor during mouse germ cell differentiation. *Mech Dev*. 1998;71(1-2):89–98. Available at: http://www.ncbi.nlm.nih.gov/pubmed/9507072.

81. Schöler HR. Octamania: the POU factors in murine development. *Trends Genet*. 1991;7(10):323–9. Available at: http://www.ncbi.nlm.nih.gov/pubmed/1781030. Accessed January 19, 2014.

82. Tantin D. Oct transcription factors in development and stem cells: insights and mechanisms. *Development*. 2013;140(14):2857–66. doi:10.1242/dev.095927.

83. Andersen B, Schonemann MD, Pearse R V, Jenne K, Sugarman J, Rosenfeld MG. Brn-5 is a divergent POU domain factor highly expressed in layer IV of the neocortex.

J Biol Chem. 1993;268(31):23390–8. Available at: http://www.ncbi.nlm.nih.gov/pubmed/7901208.

84. Taylor J, Fairburn H, Beaujean N, Meehan R, Young L. Gene expression in the developing embryo and fetus. *Reprod Suppl*. 2003;61:151–65. Available at: http://www.ncbi.nlm.nih.gov/pubmed/14635933. Accessed January 24, 2014.

85. Nakai S, Sugitani Y, Sato H, et al. Crucial roles of Brn1 in distal tubule formation and function in mouse kidney. *Development*. 2003;130(19):4751–9. doi:10.1242/dev.00666.

86. Latchman DS. POU family transcription factors in the nervous system. *J Cell Physiol*. 1999;179(2):126–33. doi:10.1002/(SICI)1097-4652(199905)179:2<126::AID-JCP2>3.0.CO;2-M.

87. Samady L, Faulkes DJ, Budhram-Mahadeo V, et al. The Brn-3b POU family transcription factor represses plakoglobin gene expression in human breast cancer cells. *Int J Cancer*. 2006;118(4):869–78. doi:10.1002/ijc.21435.

88. He X, Treacy MN, Simmons DM, Ingraham HA, Swanson LW, Rosenfeld MG. Expression of a large family of POU-domain regulatory genes in mammalian brain development. *Nature*. 1989;340(6228):35–41. doi:10.1038/340035a0.

89. Atanasoski S, Toldo SS, Malipiero U, Schreiber E, Fries R, Fontana A. Isolation of the human genomic brain-2/N-Oct 3 gene (POUF3) and assignment to chromosome 6q16. *Genomics*. 1995;26(2):272–80. Available at: http://www.ncbi.nlm.nih.gov/pubmed/7601453. Accessed January 26, 2014.

90. Rhee JM. Highly Cooperative Homodimerization Is a Conserved Property of Neural POU Proteins. *J Biol Chem*. 1998;273(51):34196–34205. doi:10.1074/jbc.273.51.34196.

91. Ishii J, Sato H, Sakaeda M, et al. POU domain transcription factor BRN2 is crucial for expression of ASCL1, ND1 and neuroendocrine marker molecules and cell growth in small cell lung cancer. *Pathol Int*. 2013;63(3):158–68. doi:10.1111/pin.12042.

92. Dominguez MH, Ayoub AE, Rakic P. POU-III Transcription Factors (Brn1, Brn2, and Oct6) Influence Neurogenesis, Molecular Identity, and Migratory Destination of Upper-Layer Cells of the Cerebral Cortex. *Cereb Cortex*. 2012:1–12. doi:10.1093/cercor/bhs252.

93. Nakai S, Kawano H, Yudate T, et al. The POU domain transcription factor Brn-2 is required for the determination of specific neuronal lineages in the hypothalamus of the mouse. *Genes Dev*. 1995;9(24):3109–3121. doi:10.1101/gad.9.24.3109.

94. Treier M, Rosenfeld MG. The hypothalamic-pituitary axis: co-development of two organs. *Curr Opin Cell Biol*. 1996;8(6):833–43. Available at: http://www.ncbi.nlm.nih.gov/pubmed/8939677. Accessed January 28, 2014.

95. Nakai S, Kawano H, Yudate T, et al. The POU domain transcription factor Brn-2 is required for the determination of specific neuronal lineages in the hypothalamus of the mouse. *Genes Dev*. 1995;9(24):3109–3121. doi:10.1101/gad.9.24.3109.

96. Wapinski OL, Vierbuchen T, Qu K, et al. Hierarchical mechanisms for direct reprogramming of fibroblasts to neurons. *Cell*. 2013;155(3):621–35. doi:10.1016/j.cell.2013.09.028.

97. Schreiber E, Himmelmann A, Malipiero U. Human small cell lung cancer expresses the octamer DNA-binding and nervous system-specific transcription factor N-Oct 3 (brain-2). *Cancer Res*. 1992;52(21):6121–4. Available at: http://www.ncbi.nlm.nih.gov/pubmed/1327524. Accessed March 25, 2014.

98. The human protein atlas. Available at: http://www.proteinatlas.org/ENSG00000184486/cell.

99. Hara Y, Rovescalli a C, Kim Y, Nirenberg M. Structure and evolution of four POU domain genes expressed in mouse brain. *Proc Natl Acad Sci U S A*. 1992;89(8):3280–4. Available at: http://www.pubmedcentral.nih.gov/articlerender.fcgi?artid=48850&tool=pmcentrez&rendertype=abstract.

100. Schreiber E, Harshman K, Kemler I, Malipiero U, Schaffner W, Fontana a. Astrocytes and glioblastoma cells express novel octamer-DNA binding proteins distinct from the ubiquitous Oct-1 and B cell type Oct-2 proteins. *Nucleic Acids Res*. 1990;18(18):5495–503. Available at: http://www.pubmedcentral.nih.gov/articlerender.fcgi?artid=332229&tool=pmcentrez&rendertype=abstract.

101. Berlin I, Denat L, Steunou A-L, et al. Phosphorylation of BRN2 modulates its interaction with the Pax3 promoter to control melanocyte migration and proliferation. *Mol Cell Biol*. 2012;32(7):1237–47. doi:10.1128/MCB.06257-11.

102. Cobrinik D, Francis RO, Abramson DH, Lee TC. Rb induces a proliferative arrest and curtails Brn-2 expression in retinoblastoma cells. *Mol Cancer*. 2006;5:72. doi:10.1186/1476-4598-5-72.

103. Bratthauer G. The avidin-biotin complex (ABC) method and other avidin-biotin binding methods. *Immunocytochemical methods Protoc*. 1999;588:257–70. doi:10.1007/978-1-59745-324-0_26.

104. Krenacs L, Krenacs T, Stelkovics E, Raffeld M. Heat-induced antigen retrieval for immunohistochemical reactions in routinely processed paraffin sections. *Methods Mol Biol*. 2010;588:103–19. doi:10.1007/978-1-59745-324-0_14.

105. Ramos-Vara J a. Technical aspects of immunohistochemistry. *Vet Pathol*. 2005;42(4):405–26. doi:10.1354/vp.42-4-405.

106. Kurien BT, Scofield RH. Western blotting. *Methods*. 2006;38(4):283–93. doi:10.1016/j.ymeth.2005.11.007.

107. NanoDrop 1000 Spectrophotometer V3.7 User's Manual. Available at: http://nanodrop.com/Library/nd-1000-v3.7-users-manual-8.5x11.pdf.

108. Image Processing and Analysis in Java Manual. Available at: http://rsb.info.nih.gov/ij/docs/menus/analyze.html#gels.

109. VanGuilder HD, Vrana KE, Freeman WM. Twenty-five years of quantitative PCR for gene expression analysis. *Biotechniques*. 2008;44(5):619–26. doi:10.2144/000112776.

110. RNeasy Mini Handbook. Available at: http://www.genome.duke.edu/cores/microarray/services/rna-qc/documents/RNeasy_Mini_Handbook.pdf.

111. Brody JR, Kern SE. History and principles of conductive media for standard DNA electrophoresis. *Anal Biochem*. 2004;333(1):1–13. doi:10.1016/j.ab.2004.05.054.

112. Die I Van. Transformation in Escherichia coli: studies on the role of the heat shock in induction of competence. *J Gen …*. 1983;129(3):663–70. Available at: http://www.ncbi.nlm.nih.gov/pubmed/6348205. Accessed May 7, 2014.

113. Fleige S, Pfaffl MW. RNA integrity and the effect on the real-time qRT-PCR performance. *Mol Aspects Med*. 2006;27(2-3):126–39. doi:10.1016/j.mam.2005.12.003.

114. Annovazzi L, Mellai M, Caldera V, Valente G, Schiffer D. SOX2 expression and amplification in gliomas and glioma cell lines. *Cancer Genomics Proteomics*. 2011;8(3):139–47. Available at: http://www.ncbi.nlm.nih.gov/pubmed/21518820.

115. Ueda R, Yoshida K, Kawakami Y, Kawase T, Toda M. Expression of a transcriptional factor, SOX6, in human gliomas. *Brain Tumor Pathol*. 2004;21(1):35–8. doi:10.1007/s10014-004-0152-3.

116. Weigle B, Ebner R, Temme A, et al. Highly specific overexpression of the transcription factor SOX11 in human malignant gliomas. *Oncol Rep*. 2005;13(1):139–44. Available at: http://www.ncbi.nlm.nih.gov/pubmed/15583815. Accessed March 22, 2014.

117. Yang Y, Niu C-S, Cheng C-D. Pin1-Nanog expression in human glioma is correlated with advanced tumor progression. *Oncol Rep*. 2013;30(2):560–6. doi:10.3892/or.2013.2481.

118. Schreiber E, Merchant RE, Wiestler OD, Fontana A. Primary brain tumors differ in their expression of octamer deoxyribonucleic acid-binding transcription factors from long-term cultured glioma cell lines. *Neurosurgery*. 1994;34(1):129–35. Available at: http://www.ncbi.nlm.nih.gov/pubmed/8121549. Accessed May 25, 2014.

119. Goodall J, Martinozzi S. Brn-2 expression controls melanoma proliferation and is directly regulated by β-catenin. *… Cell Biol*. 2004;24(7):2915–22. doi:1128/MCB.24.7.2915–2922.2004.

120. Goodall J, Wellbrock C. The Brn-2 transcription factor links activated BRAF to melanoma proliferation. ... *Cell Biol*. 2004;24(7):2923–2931. doi:10.1128/MCB.24.7.2923-2931.2004.

121. Kyritsis AP, Tsokos M, Triche TJ, Chader GJ. Retinoblastoma--origin from a primitive neuroectodermal cell? *Nature*. 307(5950):471–3. Available at: http://www.ncbi.nlm.nih.gov/pubmed/6694739. Accessed May 25, 2014.

122. Shamamian P, Mancini M. Recognition of neuroectodermal tumors by melanoma-specific cytotoxic T lymphocytes: evidence for antigen sharing by tumors derived from the neural crest. *Cancer Immunol …*. 1994;39(2):73–83. doi:10.1007/BF01525312.

123. Lyons S a, O'Neal J, Sontheimer H. Chlorotoxin, a scorpion-derived peptide, specifically binds to gliomas and tumors of neuroectodermal origin. *Glia*. 2002;39(2):162–73. doi:10.1002/glia.10083.

124. Eisen T, Easty DJ, Bennett DC, Goding CR. The POU domain transcription factor Brn-2: elevated expression in malignant melanoma and regulation of melanocyte-specific gene expression. *Oncogene*. 1995;11(10):2157–64. Available at: http://www.ncbi.nlm.nih.gov/pubmed/7478537. Accessed March 25, 2014.

125. Eisen TG. The control of gene expression in melanocytes and melanomas. *Melanoma Res*. 1996;6(4):277–84. Available at: http://www.ncbi.nlm.nih.gov/pubmed/8873046. Accessed March 26, 2014.

126. Tan C, Takayama T, Takaoka N. Impact of Gender in Renal Cell Carcinoma: The Relationship of FABP7 and BRN2 Expression with Overall Survival. *Clin Med …*. 2014;8:21–7. doi:10.4137/CMO.S13684.

127. Greenbaum D, Colangelo C, Williams K, Gerstein M. Comparing protein abundance and mRNA expression levels on a genomic scale. *Genome Biol*. 2003;4(9):117. doi:10.1186/gb-2003-4-9-117.

128. Maier T, Güell M, Serrano L. Correlation of mRNA and protein in complex biological samples. *FEBS Lett*. 2009;583(24):3966–73. doi:10.1016/j.febslet.2009.10.036.

129. Suvà ML, Rheinbay E, Gillespie SM, et al. Reconstructing and Reprogramming the Tumor-Propagating Potential of Glioblastoma Stem-like Cells. *Cell*. 2014;157(3):580–94. doi:10.1016/j.cell.2014.02.030.

130. Tanaka S, Kamachi Y. Interplay of SOX and POU factors in regulation of the Nestin gene in neural primordial cells. ... *Cell Biol*. 2004;24(20):8834–46. doi:10.1128/MCB.24.20.8834-8846.2004.

131. Baranek C, Sock E, Wegner M. The POU protein Oct-6 is a nucleocytoplasmic shuttling protein. *Nucleic Acids Res*. 2005;33(19):6277–86. doi:10.1093/nar/gki947.

132. Cook AL, Donatien PD, Smith AG, et al. Human melanoblasts in culture: expression of BRN2 and synergistic regulation by fibroblast growth factor-2, stem cell factor, and

endothelin-3. *J Invest Dermatol*. 2003;121(5):1150–9. doi:10.1046/j.1523-1747.2003.12562.x.

133. Thomson JA, Murphy K, Baker E, et al. The brn-2 gene regulates the melanocytic phenotype and tumorigenic potential of human melanoma cells. *Oncogene*. 1995;11(4):691–700. Available at: http://www.ncbi.nlm.nih.gov/pubmed/7651733. Accessed March 25, 2014.

134. Ke LD, Shi Y-X, Yung WKA. VEGF(121), VEGF(165) overexpression enhances tumorigenicity in U251 MG but not in NG-1 glioma cells. *Cancer Res*. 2002;62(6):1854–61. Available at: http://www.ncbi.nlm.nih.gov/pubmed/11912165. Accessed April 4, 2014.

135. Ohgaki H, Kleihues P. Genetic alterations and signaling pathways in the evolution of gliomas. *Cancer Sci*. 2009;100(12):2235–41. doi:10.1111/j.1349-7006.2009.01308.x.

9. APPENDIX

9.1 IHC staining for 51 samples of glioma with different grades

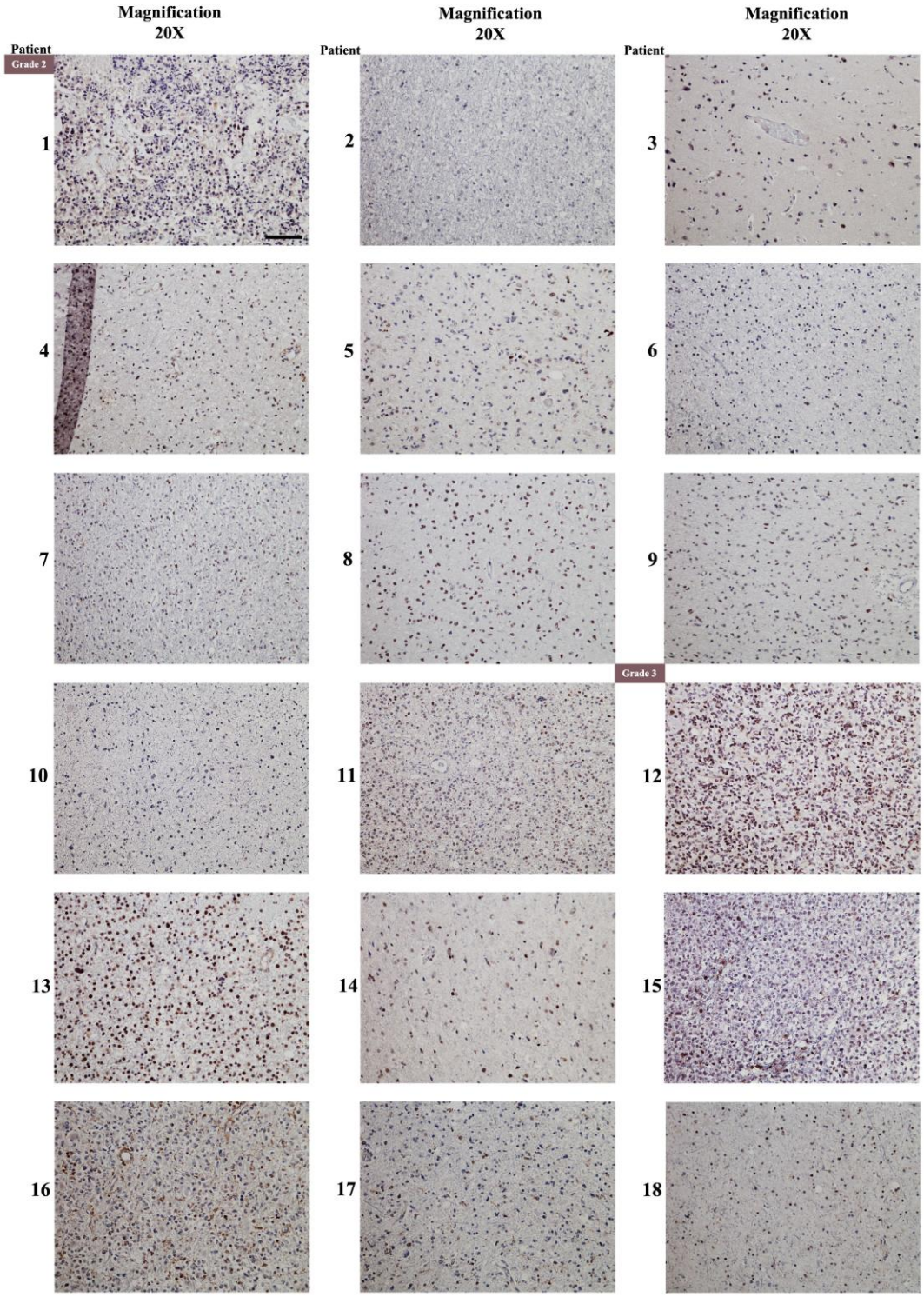

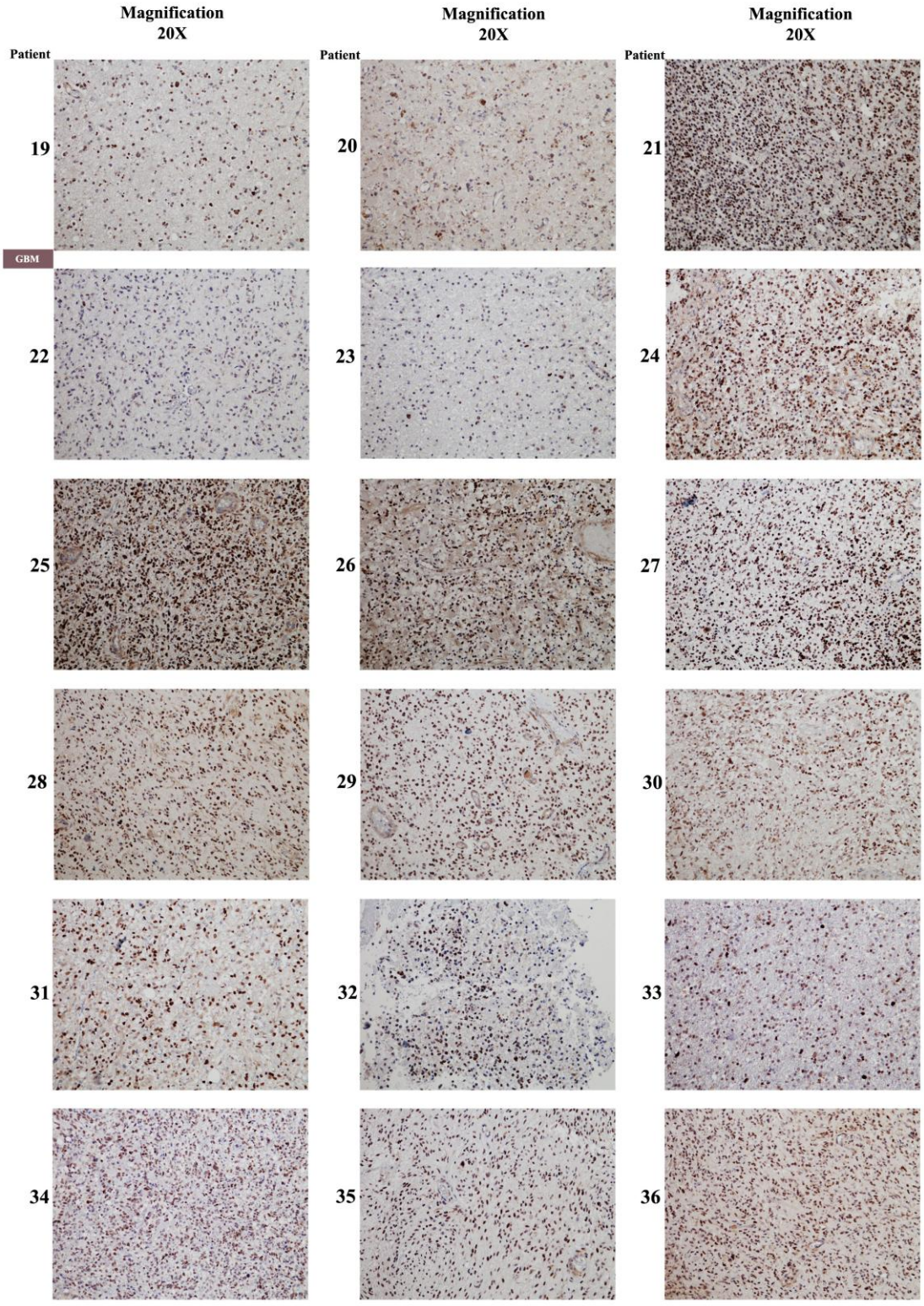
Magnification
20X
Patient
19
Magnification
20X
Patient
20
Magnification
20X
Patient
21
GBM
22
23
24
25
26
27
28
29
30
31
32
33
34
35
36

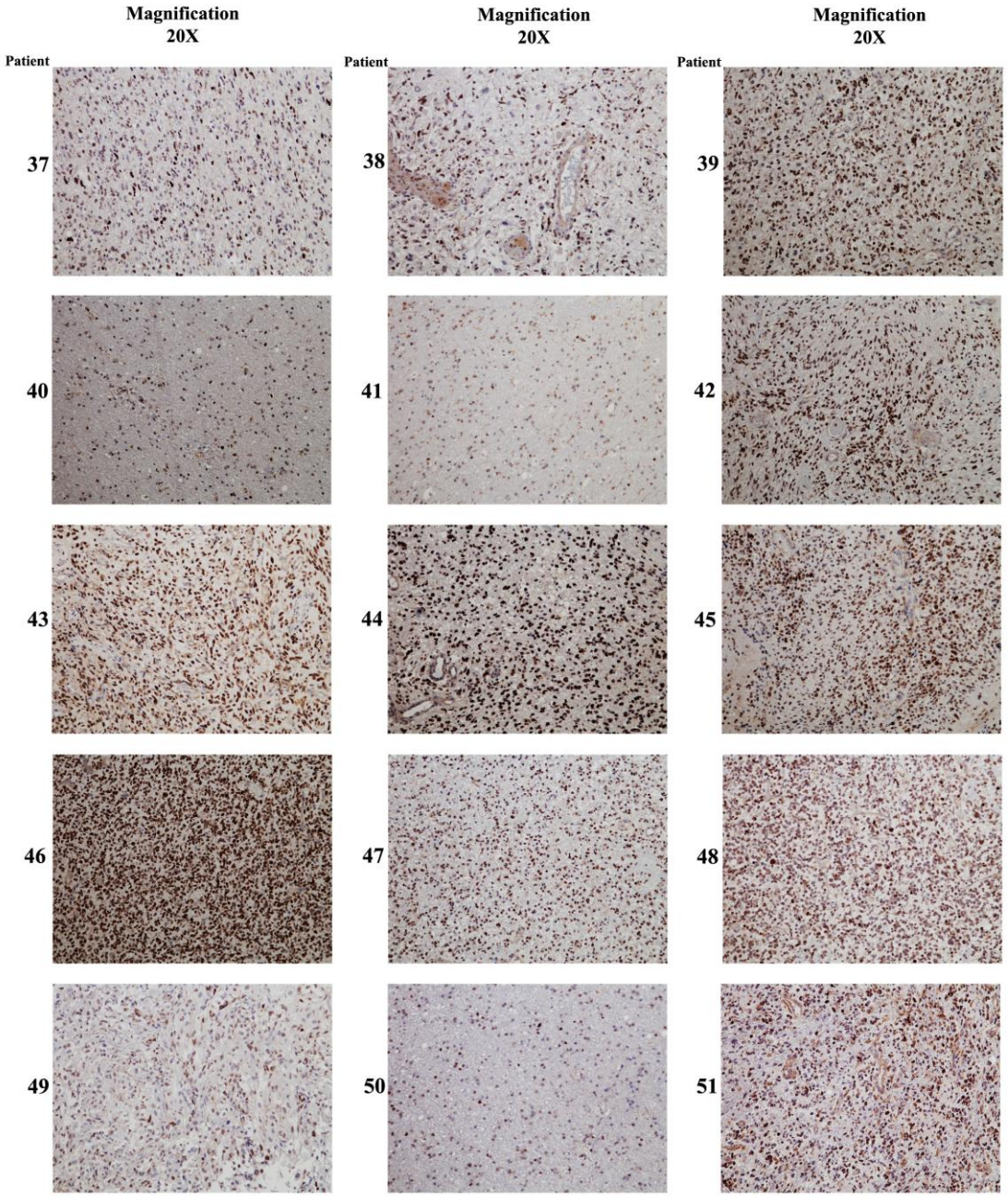

Figure 9.1 All the stained samples with IHC staining for grade II, III and IV: Different grades stained against POU3f2 antibody. All the pictures are shown with 20x magnification, scale bar = 100µm;